THESIS FOR THE DEGREE OF DOCTOR OF PHILOSOPHY

IN

MACHINE AND VEHICLE SYSTEMS

Numerical and Experimental Investigations on Aerodynamic and Thermal Aspects of Rotating Wheels

ALEXEY VDOVIN

Department of Applied Mechanics
CHALMERS UNIVERSITY OF TECHNOLOGY
Gothenburg, Sweden, 2015

Numerical and Experimental Investigations on Aerodynamic and Thermal Aspects of Rotating Wheels

A L E X E Y V D O V I N

ISBN 978-91-7597-246-6

Doktorsavhandlingar vid Chalmers tekniska högskola
Ny serie nr 3927
ISSN: 0346-718X

Department of Applied Mechanics
Chalmers University of Technology
SE-412 96 Gothenburg
Sweden
Telephone +46 (0)31 772 1000

Cover: Stylized thermal camera image from the wind tunnel test

Printed by Chalmers Reproservice
Göteborg, Sweden 2015

Numerical and Experimental Investigations on Aerodynamic and Thermal Aspects of Rotating Wheels

Alexey Vdovin
Department of Applied Mechanics
Chalmers University of Technology

Abstract

With todays and future environmental legislations for CO_2 and other emission gases, all vehicle manufacturers are forced to further develop tools and methods to make their vehicles more energy efficient and environmentally friendly. One option to achieve this is to reduce the aerodynamic resistance since it has a significant influence on the vehicle fuel consumption, especially for velocities higher than 50 km/h.

Several methods can be used to assess the aerodynamic performance of passenger cars. Wind tunnel testing and numerical simulations are two of the most common, and both have evolved considerably over the last decades. Moreover, growing computational capacity and increasing general knowledge on the methods in context allow the vehicle manufacturers to advance even further in the development of their products. Hence, some effects, phenomena and processes, not accounted for earlier, can be studied thoroughly today.

In this thesis a number of such effects and phenomena associated with rotating wheels of a passenger vehicle are addressed. The discussions focus on three main topics: deformation of tyres under different driving and testing scenarios; wheel aerodynamic resistance moment also known as ventilation resistance; and the possibility of combining aerodynamics and thermal management on studies of brake system performance. All topics are investigated experimentally in the Volvo aerodynamic wind tunnel as well as numerically using CFD simulations.

From the results it can be concluded that the wheel ventilation resistance moment has a significant influence on the total aerodynamic resistance of a vehicle; however, both measurements and computations of this moment are quite challenging. Furthermore, it has been found that the inertial expansion of tyres is responsible for a substantial change in vehicle ride height and pitch angle. These movements are often restricted in wind tunnel studies, but can be captured using different types of fastening struts that allow vertical displacements, also known as floating struts. It has been shown that that there is a significant difference in the aerodynamic forces measured depending on the type of strut being used during the test. This is especially pronounced at high velocities. Lastly, the investigation has shown a large potential in combining aero- and thermodynamics for modelling and studying of the brake system performance under different load scenarios. However, further investigations are required to extend and develop the current simulation model.

Keywords: vehicle aerodynamics, ventilation resistance, aerodynamic moment, wind tunnel, CFD, rim design, ride height, brake cooling.

Acknowledgements

This work would not have been possible without the support from a large group of individuals. Therefore, I would like to take the opportunity to acknowledge them here.

The research was carried out at the division of Vehicle Engineering and Autonomous Systems at Chalmers University of Technology and it was funded by the Swedish Energy Agency. The experimental investigations were conducted at the Volvo Car Corporation aerodynamic wind tunnel and the numerical simulations were mostly carried out using resources provided by the Swedish National Infrastructure for Computing (SNIC).

I would like to express my gratitude to my supervisors, Professor Lennart Löfdahl from Chalmers and Dr. Simone Sebben from Volvo Car Corporation, for giving me this great opportunity to work as a Ph.D. student with such an interesting topic as Road Vehicle Aerodynamics. Their feedback and guidance helped me a lot during my studies. Here I would also like to acknowledge Mr. Tim Walker whose experience contributed greatly to the project and increased the quality of this work.

Thank you to all managers and engineers from Aerodynamics, Thermodynamics and Brakes groups at Volvo Car Corporation, especially to Torgny Karlsson and Alexander Broniewicz, for support with everyday issues, wonderful atmosphere and productive discussions. Same thank you goes to all technicians from Volvo who helped me prepare and carry out numerous wind tunnel tests.

At Chalmers I would like to express my appreciation to some former Ph.D. students and research engineers in the Road Vehicle Aerodynamics research group: Dr. Christoffer Landström, Dr. David Söderblom, Dr. Peter Gullberg, Dr. Lasse Christoffersen, Dr. Jesper Marklund, Dr. Lisa Henriksson, Dr. Lennert Sterken, as well as Andrew Dawkes, Johan Zaya, Daryosh Farin and Jonathan Rice. All of them supported me in the beginning of my Ph.D. studies and made a lot of things easier and less stressful. I am also thankful to the current members of the RVAD group: Teddy Hobeika, Blago Minovski, Sabine Bonitz, Helena Martini and Emil Ljungskog. They created a great working atmosphere, contributed to my research and helped me with numerous big and small challenges.

Finally, I would like to thank my dear family and friends for their constant support and encouraging during my studies at Chalmers. Special thank you is addressed to my fiancée, Natalia Mokhnacheva, who brought love into my life and made my last years of Ph.D. studies better in so many ways.

Göteborg, 2015
Alexey Vdovin

List of Publications

This thesis concludes the research carried out at Chalmers University of Technology from 2011 to 2015. The thesis is based on the following publications, referred to in the text by Roman numbers:

I. Vdovin, A., Bonitz, S., Landstrom, C. and Lofdahl, L., "Investigation of Wheel Ventilation-Drag using a Modular Wheel Design Concept," SAE Int. J. Passeng. Cars - Mech. Syst. 6(1):2013, doi:10.4271/2013-01-0953.

II. Vdovin, A., Lofdahl, L., and Sebben, S., "Investigation of Wheel Aerodynamic Resistance of Passenger Cars," SAE Int. J. Passeng. Cars - Mech. Syst. 7(2):2014, doi:10.4271/2014-01-0606.

III. A. Vdovin, L. Löfdahl, S. Sebben and T. Walker, "Investigation of vehicle ride height and wheel position influence on the aerodynamic forces of ground vehicles," in International Vehicle Aerodynamics Conference 2014, Loughborough, UK, 2014.

IV. A. Vdovin, L. Löfdahl and S. Sebben, "Numerical and Experimental Investigations of Brake Cooling for Passenger Cars," in European Conference - Thermal Systems And Aerodynamic Solutions For Ground Vehicles, Torino, Italy, 2015.

V. A. Vdovin, T. Hobeika, L. Löfdahl and S. Sebben, "Numerical Investigations of Aerodynamic Resistance Moments of Rotating Wheels on Passenger Cars," submitted to SAE Int. J. Passeng. Cars - Mech. Syst., 2015.

Division of work between authors

The author of this thesis produced the results and wrote all manuscripts with the exceptions explicitly mentioned in this section. All corresponding co-authors have provided valuable contributions in terms of revising the content of the work and resulting papers. The work presented in Paper I was based on the master thesis by Sabine Bonitz [1]. Analysis of the results was performed by Sabine Bonitz and Alexey Vdovin, and the writing of the manuscript was carried out by the author. The simulations for Paper V were conducted by Teddy Hobeika, analysis of the results and writing of the paper were done by Alexey Vdovin.

Other relevant publications

- A. Vdovin, L. Löfdahl, C. Landström, “Aerodynamic Wheel Force Measurements on a Detailed Scale-Model Car – Possibilities and Challenges”, 8th International Symposium on Strain-Gauge Balances, 7-10 May, Lucerne, Switzerland, 2012;

- A. Vdovin, "Investigation of Aerodynamic Resistance of Rotating Wheels on Passenger Cars," *Thesis for Licentiate of Engineering*, Gothenburg, Chalmers, 2013.

- T. Hobeika, A. Vdovin and L. Löfdahl, "Influence of Rims and Tyres on the Aerodynamic Resistance of Passenger Vehicles," in *Haus der Technik*, München, Germany, 2014;

- L. Löfdahl, T. Hobeika, A. Vdovin, "On the Aerodynamic Performance of Two Silver Arrows from the Thirties", in *15. Internationales Stuttgarter Symposium: Automobil- und Motorentechnik*, Stuttgart, Germany, 2014.

Nomenclature

Symbols

A	Projected front area	[m^2]
C_D	Aerodynamic drag coefficient	[-]
$C_{D(AD)}$	Aerodynamic drag coefficient	[-]
$C_{D(vent)}$	Ventilation drag coefficient	[-]
$C_{D(Tot)}$	Total aerodynamic resistance coefficient	[-]
f_r	Rolling resistance coefficient	[-]
g	Gravitational acceleration	[m/s^2]
F_{drag}	Aerodynamic drag force	[N]
F_D	Aerodynamic drag force	[N]
F'_D	Total aerodynamic drag force (including ventilation drag)	[N]
$f_{inertia}$	Distributed inertial forces due to rotation of the masses	[N/m^3]
F_{lift}	Aerodynamic lift force	[N]
F_{trac}	Traction force	[N]
F'_{trac}	Part of the traction force, responsible for ventilation resistance	[N]
F_{vent}	Equivalent ventilation resistance force	[N]
F_x	Driving resistance	[N]
F_{x_mech}	x-component of the equivalent mechanical force	[N]
F_{z_mech}	z-component of the equivalent mechanical force	[N]
m	Mass of vehicle	[kg]
M_{air}	Aerodynamic resistance moment	[Nm]
$M_{inertia}$	Resistance moment due to inertia of the rotating parts	[Nm]
M_{y_mech}	Equivalent mechanical moment around y-axis	[Nm]
M_{vent}	Ventilation moment	[Nm]
P_{vent}	Power required to overcome ventilation resistance	[W]
V	Absolute vehicle velocity	[m/s]
V_{rel}	Vehicle velocity relative to air	[m/s]
α	Road inclination	[deg]
γ	Coefficient including the inertia of rotating parts	[-]
ρ	Air density	[kg/m^3]
ω	Rotational velocity	[rad/s]

Abbreviations

CAD	Computer-aided Design
CFD	Computational Fluid Dynamics
EU	European Union
NEDC	New European Driving Cycle
MRF	Multiple Reference Frame
OICA	International Organization of Motor Vehicle Manufacturers (“Organisation Internationale des Constructeurs d’Automobiles”)

WLTC	Worldwide harmonized Light vehicles Test Cycle
WLTP	Worldwide harmonized Light vehicles Test Procedures
WDU	Wheel Drive Unit

Table of Contents

Part I
Extended Summary

1. Introduction

1.1. Background

Passenger cars are an important part of a modern world life, and nowadays it is hard to imagine our life without them. They provide a convenient way of travelling and commuting, especially in the regions where access to a good public transportation network is limited. As the population of Earth grows, so does the demand for personal transportation. According to the statistics from the International Organization of Motor Vehicle Manufacturers (OICA) there were more than 67 million passenger vehicles produced in the world just in 2014, see Figure 1.

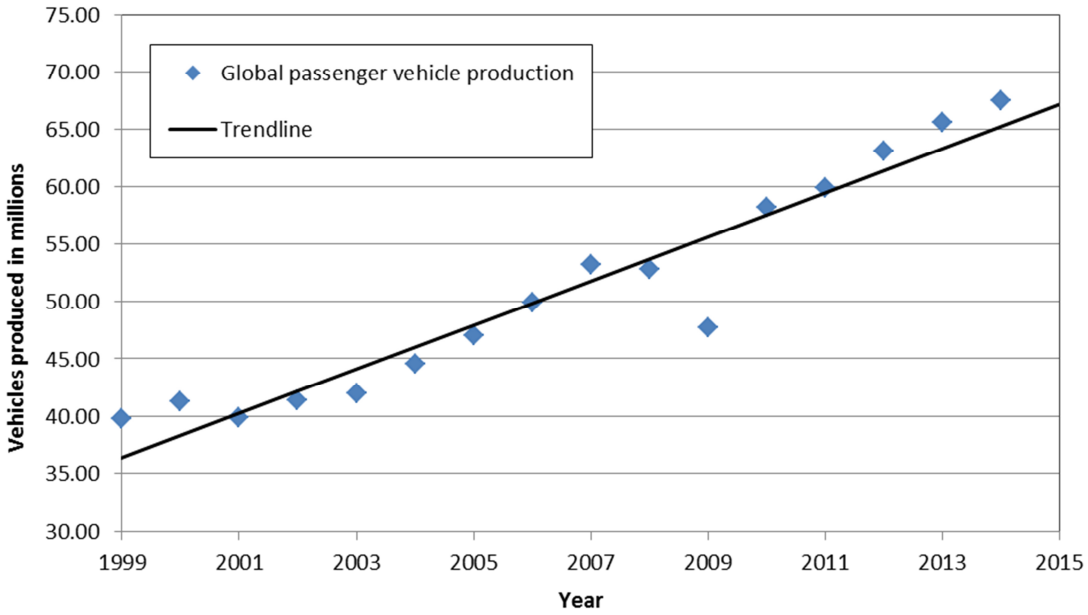

Figure 1. Global passenger vehicle production in millions [2]

Most of these vehicles are powered by internal combustion engines and therefore it is hard to ignore the environmental issues associated with this. The emissions produced as a side product of a combustion process can have negative effects on our planet. The main concern in this case is carbon dioxide (CO_2), which is an important greenhouse gas. It is considered to be the reason for anthropogenic climate change in terms of causing global warming. Road transportation is accountable for about 16% of man-made CO_2 emissions, compared to about 44% produced in the process of electricity generation and about 18% in manufacturing and production [3]. Nevertheless, there is a huge pressure on vehicle manufacturers to produce more environmentally-friendly cars.

The European Union sets mandatory emission reduction targets for all new cars. The law requires that the fleet average CO_2 emissions per kilometre for every manufacturer should be below 130 grams at this moment, and by the year 2021 this number should be lowered to just 95 g/km. This means that of a vehicle produced in 2020 should burn around 4.1 per 100 km of petrol or 3.6 per 100 km of diesel [4]. The EU is not unique in its campaign for fuel efficient and environmentally friendly vehicles: USA, China, India, Japan and other countries worldwide are also promoting similar regulations.

In order to measure the fuel consumption and CO_2 emissions of a vehicle, car manufacturers are using complex test procedures also known as "driving cycles" that combine multiple driving scenarios. In EU the New European Driving Cycle (NEDC) is currently used, but the ability of this cycle to represent real-world driving conditions is widely debated [5]. A new procedure called "Worldwide harmonized Light vehicles Test Procedure" (WLTP) is currently being developed in cooperation between EU, Japan and India [6]. It is mandated in the EU that WLTP will replace NEDC in 2017. This new procedure consists of 3 different test cycles (WLTCs) that are applied depending on a vehicle class defined by power-weight ratio. Most common passenger vehicles belong to Class 3. The comparison on the WLTC Class 3 and old NEDC can be seen in Figure 2.

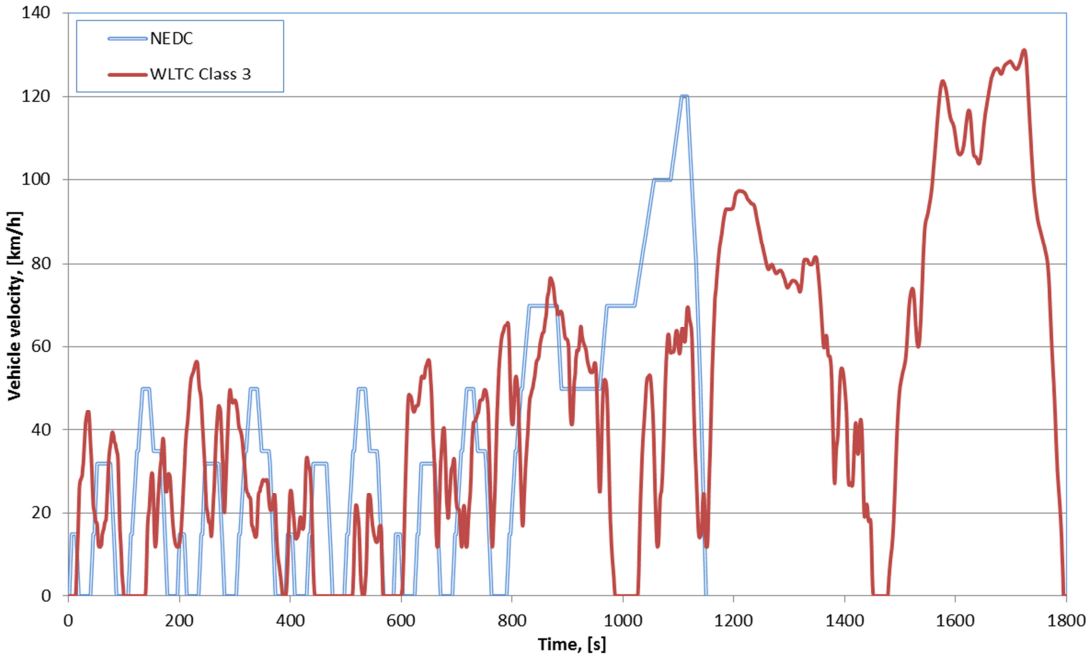

Figure 2. Comparison of two driving cycles [7, 8]

In addition to driving cycles a lot of development is going on in the areas of vehicle testing and simulating. Development of computers and simulation software allows complex numerical investigations of different processes affecting the vehicle with constantly increasing accuracy. Similar trend can be seen with experimental facilities that become more and more advanced.

1.2. Improving vehicle efficiency and aerodynamic drag

To be able to produce a more energy efficient vehicle it is required to have a good understanding of the driving resistance. Driving resistance is the total resistance force acting on the vehicle when it is moving. Usually this force is expressed using equation 1.1 [9]:

$$F_x = \gamma ma + f_R mg\cos\alpha + mg\sin\alpha + \frac{1}{2}C_D A\rho V_{rel}^2 \qquad (1.1)$$

The first term here (γma) is vehicle mass multiplied by vehicle acceleration; it represents driver behaviour in terms of acceleration or deceleration. Coefficient γ is used to take into account the inertia of rotating parts, e.g. wheels, flywheel, shafts, gears etc. The second term ($f_R mg\ cos\ \alpha$) is the rolling resistance, as can be seen it is proportional to the normal force between the tyres and the road (α is an inclination angle of the road). f_R here is a coefficient of rolling resistance which depends on wheel and road properties, and some other factors. Quite often it is assumed to be constant in relation to vehicle velocity for simplicity reasons. The third term in the equation ($mg\ sin\ \alpha$) characterizes the part of gravitational force that acts on a vehicle when going uphill or downhill and the last one ($\frac{1}{2} C_D A \rho V_{rel}^2$) is usually denoted as aerodynamic drag force or simply aerodynamic drag.

As can be seen, aerodynamic drag force is proportional to air density ρ and the square of a relative velocity between the vehicle and the air (V_{rel}). Another component of the equation is reference area A, which is the projected frontal area of the vehicle. The last term here, C_D, is an aerodynamic drag coefficient of the vehicle. It is a dimensionless factor that mainly depends on the general shape of the vehicle and can vary from 0.5 – 1 for early vehicles down to values around 0.18 – 0.24 for modern aerodynamically optimised vehicles [10, 11]. C_D is usually measured in drag counts, where one drag count is equal to a change of 0.001 in C_D. Often when comparing two vehicles a drag factor is used, which is a product of frontal area and drag coefficient ($C_D A$). It allows easy comparison of aerodynamic characteristics for vehicles with different size and shape.

Assuming level road and constant velocity of the vehicle the equation for driving resistance 1.1 can be simplified to the following form:

$$F_x = f_R mg + \frac{1}{2} C_D A \rho V_{rel}^2 \tag{1.2}$$

For a typical medium-sized European passenger vehicle, the aerodynamic drag force becomes dominant over the rolling resistance force at around 60-70 km/h, as seen in Figure 3 [9]. This means that at highway speeds the aerodynamic drag becomes the most important contributor to driving resistance and, hence, by improving the aerodynamic properties of the vehicle increased energy efficiency can be achieved.

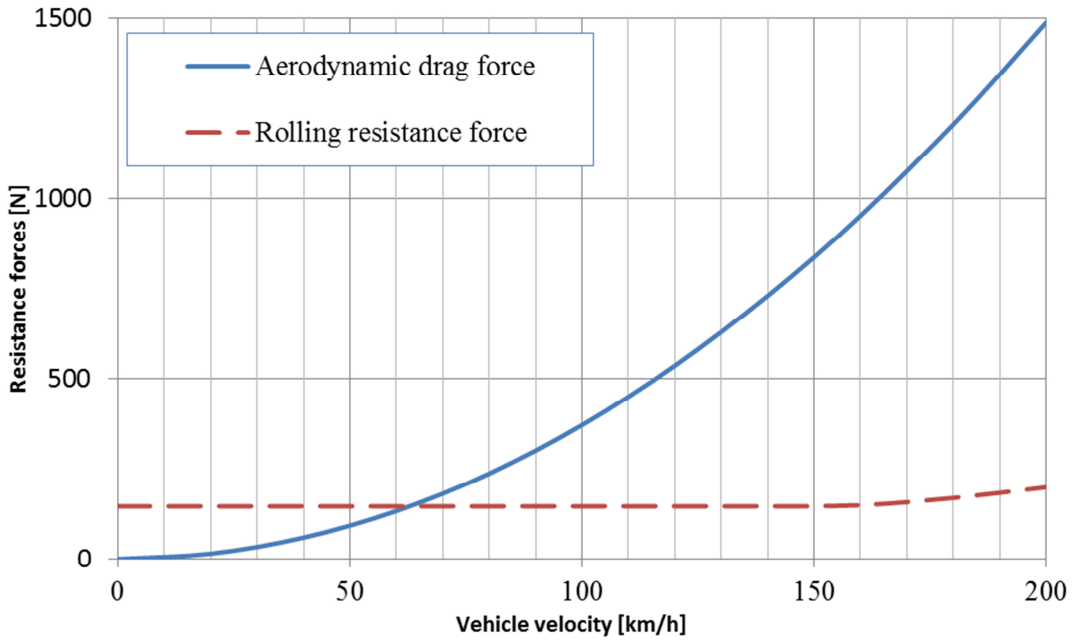

Figure 3. Aerodynamic drag force and rolling resistance force for a typical passenger vehicle

However, it should be noted that vehicles need to accelerate and decelerate, moreover they are not travelling at high speeds most of the time. Using NEDC it has been shown that the vehicle mass has a larger influence on the fuel consumption, compared to aerodynamic drag. Reducing the aerodynamic drag force by 10% for a large European passenger vehicle like Audi A8 can lead to fuel savings of around 2% [12]. For a smaller vehicle the relative fuel savings can be as high as 8%. Compared to NEDC the WLTP has increased maximum and average speeds and also reduced idle phases. These factors will result in increased influence of the aerodynamic drag in WLTP by about 50% compared to NEDC [13].

1.3. Passenger vehicle aerodynamics

Even though aerodynamics has major influence on top speed and emissions, there are other technical areas where it must be considered. Most of them are summarised in the following list:

- Performance
  - Fuel consumption
  - Emissions
  - Maximum velocity
  - Acceleration capabilities
- Cooling
  - Engine
  - Transmission
  - Brakes
  - Condenser
  - Batteries
- Comfort
  - Ventilation
  - Heating

    - Air conditioning
    - Wind noise
- Stability
    - Directional stability
    - Cross-wind sensitivity
- Visibility
    - Dirt deposition
    - Splash and spray
    - Wiper lift-off

In addition to the areas mentioned there are also other related factors like packaging of the engine bay and underbody, styling of the vehicle, etc. All of these areas and factors will influence the final external design of the vehicle and consequently will have an effect on aerodynamic drag.

Aerodynamic drag of any object can be divided into friction drag and pressure drag. The first one comes from the friction between body surface and fluid, while the second one originates from the pressure differences created around the body when surrounded by moving flow. For a relatively bluff body like a passenger vehicle, pressure drag dominates over friction drag and therefore passenger vehicles are often considered to be Reynolds independent, meaning that the drag force of a vehicle body is not changing with the air velocity [12]. This would be the case if the vehicle body was completely rigid, but with the development of the ground simulation systems in wind tunnels, it is becoming possible to capture different changes to the shape of the vehicle and resulting changes in drag and lift forces.

1.4. Ground simulation

Figure 4 shows an approximate percentage distribution of aerodynamic drag originating from different areas of importance. It has been shown that upper body shape is responsible for about 45-50% of the drag force [12, 14]. The underbody can be accounted for about 30%. While the upper body shape is largely limited by the design of the vehicle, aerodynamicists have much more freedom in improving the underbody, for example by using special panels or wheel deflectors [15, 16]. Lastly, it was found that wheels and wheelhouse flows generate up to a quarter of the aerodynamic drag force [14, 17]. A large portion of this drag comes directly from the rotating wheels and the wakes they create, but there are also important interference effects with the underbody flow and most importantly with the wake behind the vehicle [18, 19, 20].

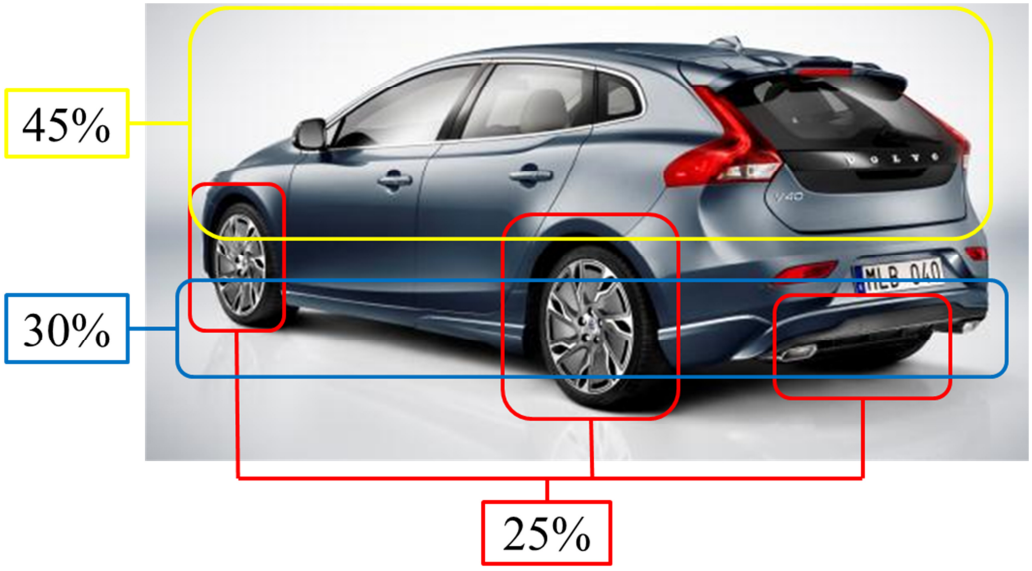

Figure 4. Contributions to the aerodynamic drag from different parts of a passenger car

Since the underbody and wheelhouses together are responsible for the largest part of the aerodynamic drag force, a significant attention is paid to capturing the correct road boundary conditions in the automotive wind tunnels [21]. In the past wind tunnels had completely stationary ground, however, nowadays these wind tunnels are being upgraded and all new ones come equipped with a number of ground simulation systems [22, 23, 24, 25, 26, 27]. These systems usually include suction scoop and distributed suction zones, designed to minimize the thickness of the oncoming boundary layer; tangential blowing slots, used to accelerate the flow next to the ground; and, most importantly, the moving ground unit, which usually comes in the form of running belts to replicate the road moving under the vehicle.

Figure 5 demonstrates four most commonly used moving ground system types. First and one of the oldest [28] is the single belt design, also referred to as full-width belt, which is often used in the model-scale wind tunnels or in racing cars development. The largest drawback of this system is that the vehicle and wheels need to be suspended from the top or from the sides by means of a stings and struts that can have serious interference effects on the airflow and consequently the forces measured [29, 30]. The remaining three systems in Figure 5 do not use the full-width bel; instead, a number of moving belts are used. This allows having a vehicle supported by means of underbody vehicle struts, which produce much less interference effects and require no modification to the vehicle body compared to a single belt setup.

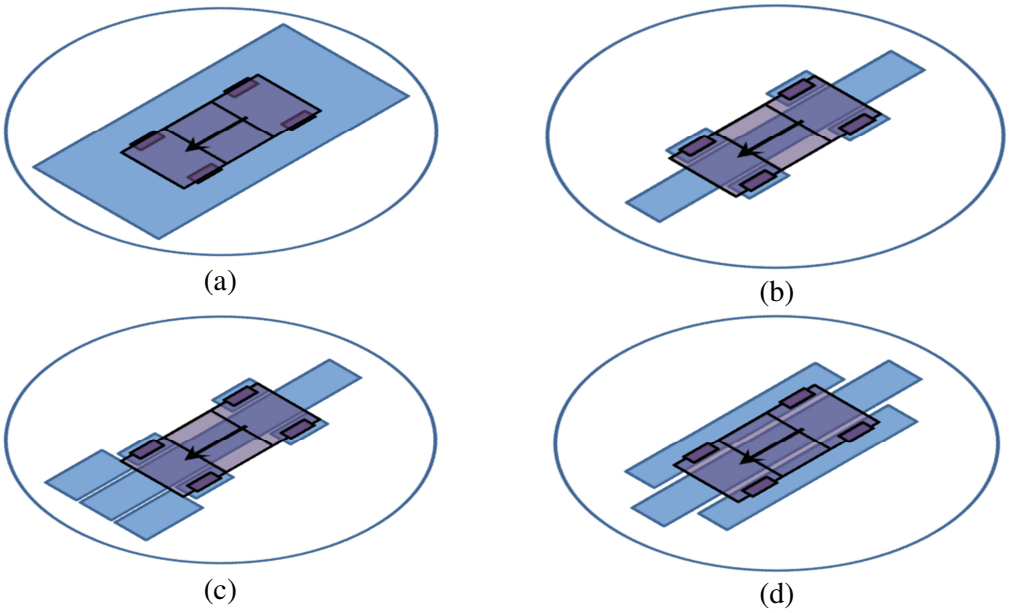

Figure 5. Different designs of a moving ground system: (a) Single belt, (b) 5-belt, (c) T-belt, (d) 3-belt.

1.5. Wheel aerodynamics

Wheels of passenger vehicles usually consist of pneumatic tyre and rim. Both of these parts can have a significant influence on the aerodynamic drag and lift.

There are a number of investigations comparing rim designs and the way they affect the drag and lift of the vehicle. It has been shown that the design of a wheel rim has a large influence not only on a local wheelhouse flow but also on the underbody and cooling flow and the base wake of the vehicle [18, 31, 32]. Rims with larger covered areas were found to be more favourable in terms of aerodynamic drag; moreover optimising the rear rims design has larger potential in decreasing the aerodynamic resistance of the vehicle [33, 34].

Tyres are equally important for the aerodynamics of the vehicle. Since the tyres are mainly made of rubber they deform significantly under the influence of vehicle weight and distributed inertial forces or centrifugal forces that are acting on them when the vehicle is moving [35]. This means that not only the shape of the tyre varies with velocity but also the relative height of the wheel axle changes. Figure 6 shows three different deformation types that occur to the rotating tyre. Depending on the type of fastening struts used, these deformations can be different and also the ride height may change, therefore force coefficients measured can be different. This is one of the topics investigated in this thesis.

Another area where tyres are extremely important is the numerical simulation of wheel rotation. Nowadays, Computational Fluid Dynamics (CFD) simulations are often used by vehicle manufacturers to complement the wind tunnel tests and sometimes to completely replace them. Recent constant computer and software development allowed not only to simulate certain parts and areas but to have full vehicle simulated in a virtual wind tunnel with a high level of detail. However, it should be noted that current level of development does not allow direct numerical simulations of the airflow around the vehicle and for any

other simulation a compromise needs to be found between the accuracy required and the computational power used.

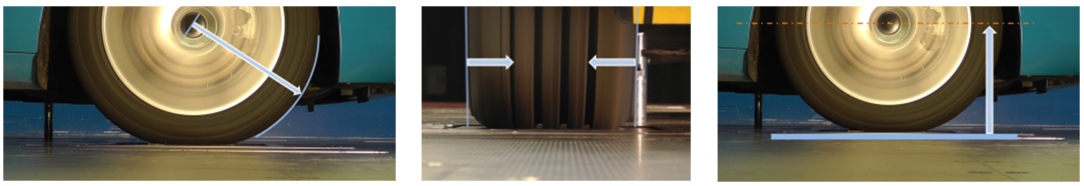

(a) (b) (c)

Figure 6. Tyre deformations due to inertial forces: (a) radial expansion; (b) axial compression; (c) vertical lift.

One of the simplifications that is usually applied when doing aerodynamic vehicle simulation is a simplified wheel rotation. A number of investigations of methods for simulating wheel rotation showed the effects of tyre pattern detail and the importance of correct modelling of the deformations in the contact patch area [36, 37, 38]. Nowadays, the most common approach to the simulated wheel rotation is to use moving wall boundary condition for the tyre and apply Multiple Reference Frame technique for the spokes, but as the technology develops more focus is put on better simulation methods.

1.6. Aerodynamic resistance moment of the wheel

As discussed previously, rotating wheels have a significant contribution to the aerodynamic drag force of the vehicle, both directly and indirectly. Furthermore, there is another aerodynamic resistance that is acting on all vehicle parts that rotate – aerodynamic resistance moment, also known as "ventilation resistance" or "pumping losses". Figure 7 shows a 2-dimensional picture of the wheel with forces and moments acting on it. As it can be seen, aerodynamic resistance moment (ventilation resistance moment), as one of many resistance moments, is counteracting wheel rotation.

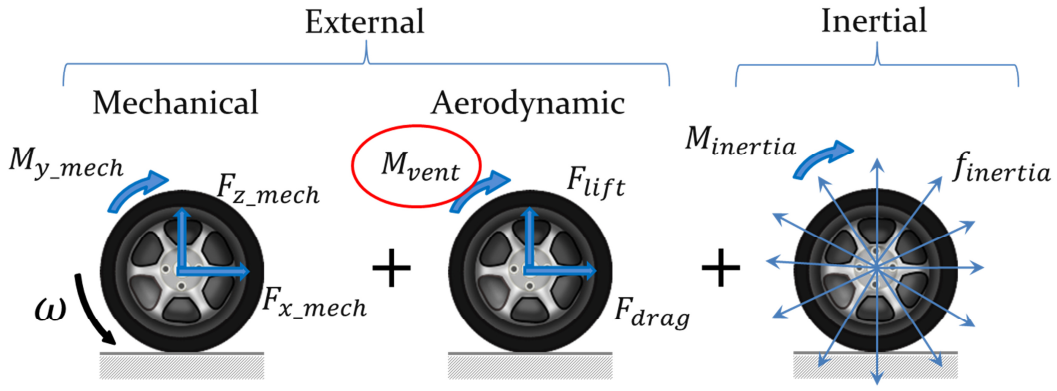

Figure 7. Forces acting on a rotating wheel

This ventilation resistance moment is originating from the fact that a rotating wheel is moving in the air, but since it is not a force it is usually unaccounted for in the aerodynamic drag coefficient. Moreover, it is often not even measured in the wind tunnels. The challenge here is that in order to measure this moment a certain modification to the wind tunnel setup is required. Knowing the moment and the rotational velocity of the wheel, one can calculate the amount of power that is required to overcome the

ventilation resistance, and therefore it is possible to account for the aerodynamic resistance moment using an equivalent drag force F_{vent}, which can be added as an extra term to the driving resistance force equation (1.1):

$$F_x = \gamma ma + f_R mg\cos\alpha + mg\sin\alpha + \frac{1}{2}C_D A\rho V_{rel}^2 + F_{vent} \tag{1.3}$$

This equivalent force can be written in the same form as the aerodynamic drag:

$$F_{vent} = \frac{1}{2}C_{D(vent)} A\rho V_{rel}^2 \tag{1.4}$$

where $C_{D(vent)}$ will be referred to as ventilation drag coefficient. The equation (1.3) in this case can be rewritten as follows:

$$F_x = \gamma ma + f_R mg\cos\alpha + mg\sin\alpha + \frac{1}{2}\left(C_{D(AD)} + C_{D(vent)}\right) A\rho V_{rel}^2 \tag{1.5}$$

Letters "AD" are added to here to aerodynamic drag coefficient to easier distinguish it from the ventilation drag one.

It has been shown both experimentally and numerically that with a certain modification to the rim design the ventilation resistance moment of the wheels can be considerably reduced. Moreover this resistance moment should not be studied separately, since modification of the rims affects the aerodynamic drag of the vehicle; instead, the sum of $C_{D(AD)} + C_{D(vent)}$ should be monitored [39, 40].

Similarly to aerodynamic drag force, ventilation resistance moment can be divided into two components: pressure and viscous. The pressure component is produced by the non-uniform normal pressure distribution around the wheel and the viscous component is originating from the surface friction acting on different rotating parts. In the case of the wheel these parts are: the tyre, the rim, and the brake disc, see Figure 8.

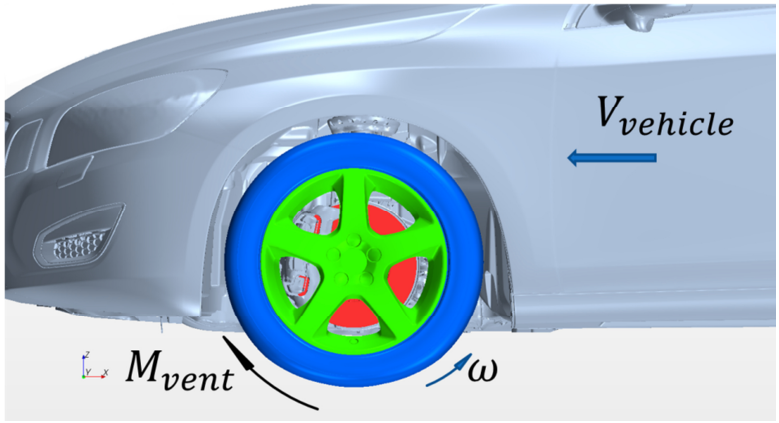

Figure 8. Main contributors to the aerodynamic resistance moment of the wheel

A large portion of this thesis is devoted to the aerodynamic resistance moment investigations. The ways to measure it in the wind tunnel, as well as the ways to calculate it using numerical simulations, are going to be addressed.

1.7. Combining aerodynamics and thermal management

Covering a large portion of the outer part of the rim is known to be resulting in a decreased overall vehicle drag [41, 33]. As it is going to be shown in Paper I and also confirmed by other authors, covering large portions of the rim is also beneficial for decreasing the aerodynamic resistance moment of the wheels [42, 43, 39]. However, since the brakes are becoming less exposed, installing such rims can have negative effect on the brake cooling performance and therefore a compromise needs to be found.

There are many examples of studies performed in order to understand and improve the processes connected with brake system work cycle, both experimentally and by using numerical simulations. Simple simulations can model only one channel inside the brake disk [44], a sector of the disk [45, 46] or just the brake disk with some surrounding geometries [47, 48, 49], while more complex studies usually involve even more geometrical parts [50, 51]. Similar situation happens on the experimental side of brakes testing. A lot of investigations are conducted using brake dynamometer that does not allow having a correct airflow picture [44, 45, 46], even though some of the dynamometer tests may be quite advanced [47].

It has been shown that proper representation of the surrounding geometries around the brake disk is essential for capturing the correct on-road conditions [52]. Therefore, wind tunnels have been used for more detailed brake cooling investigations with either quarter of a car or a full-size vehicle [52, 51, 53].

Since the cost of the simulation CPU-hour is decreasing every year and the software products are evolving, it becomes possible to conduct more and more complex simulations. In this thesis a possibility of including brakes thermal management in the full-vehicle aerodynamic simulation is investigated. Such simulations can become extremely valuable during the design phase of the vehicle development, when the working prototype is not yet available. Paper IV is presenting the ongoing work, hence identifying important issues and limitations of the current model being developed. When finished, such model can be used not only for predicting temperatures of different parts under various load scenarios, but also as a basis for other types of simulations, e.g. thermal cracking.

1.8. Project objectives

The overall goal of this research project was to increase the understanding of wheel aerodynamics on passenger vehicles with a focus on aerodynamic resistance moment. This general goal was subdivided into specific research questions:

- How to measure the aerodynamic resistance moment in the wind tunnel?
- How different rim designs affect this moment and total aerodynamic resistance of the vehicle?
- How can the aerodynamic resistance moment be estimated using numerical simulations and what are the important factors to consider?

Since a large part of the studies was conducted in the wind tunnel and involved altered interaction between the tyre and the ground, the following additional question was investigated:

- How does the choice of supporting struts affect the tyre geometry, the vehicle positioning and the forces being measured?

Lastly, as the covered rims were found to be among the best both in terms of aerodynamic drag force and wheel resistance moments, an investigation was conducted on the brake cooling performance test, mainly answering the question:

- How can the brake test be reproduced in the wind tunnel and what is needed to replicate the same results using numerical simulation?

1.9. Outline of the thesis

Part I summarises the results of several experimental and numerical investigations on the topics:

- Drive height changes due to tyre deformation, and resulting differences in the wind tunnel measurements for different vehicle fastening strategies used;

- Aerodynamic resistance moment of the wheels and its effects on the total aerodynamic resistance of the vehicle;

- Brake cooling investigations.

The methods used for all investigations are presented in chapter 2 and the results are summarised and discussed in chapter 3. Lastly, some concluding remarks are given.

Part II consists of 5 appended papers that can provide some more details on the work conducted.

2. Methodology

The work presented in this thesis has been conducted using both wind tunnel experiments and numerical simulations; it included some pure aerodynamic investigations and also some investigations combining aerodynamics and thermal management. This chapter gives an overview of different setups that has been used for these studies, more detailed information can be found in the corresponding papers that are attached.

2.1. Test object

The test object selected for all of the investigations was a standard production sedan type vehicle: Volvo S60 equipped with 215/50 ZR17 tyres, see Figure 9. The exact vehicles in the wind tunnel were changing from test to test but the differences between them were minimised. This allowed using the same CAD model of the vehicle with only minor modifications in all of the numerical simulations, even though for some of the simulations the vehicle model was significantly simplified.

Figure 9. One of the Volvo S60 vehicles used

2.2. Wind tunnel investigations

All wind tunnel investigations presented were conducted in a Volvo aerodynamic wind tunnel. It is a full-scale closed-circuit wind tunnel with a cross sectional area of 27 m^2 and slotted wall test section. Figure 10 shows a test section layout of the wind tunnel, with different parts of the ground simulation system identified [23]. It can be seen that the tunnel is equipped with a five-belt moving ground system installed on a turntable. This system has one centre belt and four wheel drive units (WDUs). The vehicle is fixed in position by four vehicle struts; example of the vehicle installation on the balance and the geometry of the WDU are shown in Figure 11. Both the struts and the WDUs are connected to the main balance measuring the forces. This setup makes the rolling resistance force between the wheels and the belt an internal force, therefore the rolling resistance is not registered by the balance, allowing measuring just the aerodynamic loads. Nevertheless, additional load cells inside WDUs can be used to obtain the traction force produced in the contact patch of each wheel.

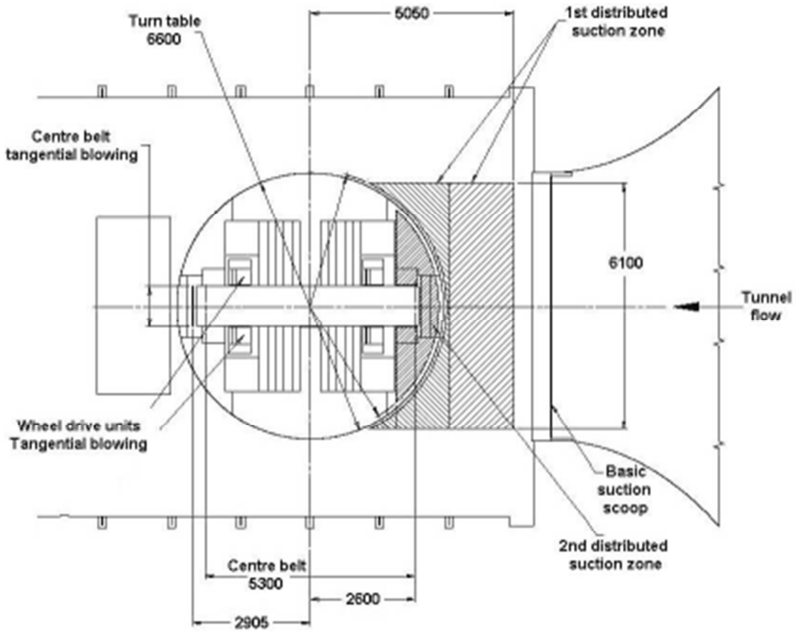

Figure 10. Overview of the ground simulation system in the Volvo aerodynamic wind tunnel [23]

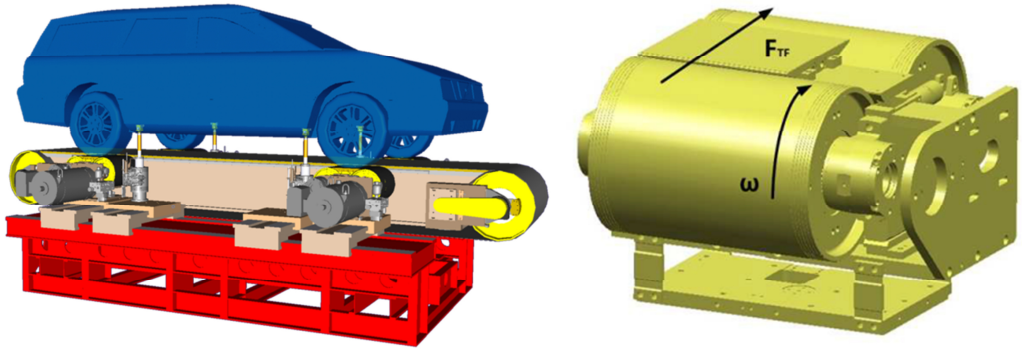

Figure 11. Test vehicle installed on a force balance and the wheel drive unit (courtesy of Volvo Car Corporation)

2.2.1 Aerodynamic resistance moment measurements

By measuring the traction force and knowing the current deformed radius of the wheel, it is possible to calculate the moment required to rotate it. Unfortunately, this moment is different from the ventilation resistance moment that needs to be measured. In addition to the aerodynamic resistance, there are other losses and resistances associated with the rotating wheel. To measure the moment in question, one needs to isolate the part of the traction force that is responsible for overcoming the ventilation resistance moment, hence the following resistances need to be removed or estimated:

- Rolling resistance moment
- Inertial resistance moment
- Losses in bearings
- Losses in brakes
- Losses associated with drive-shaft and gearbox
- Losses due to slip in a contact patch of the wheel

In addition, the temperature of the tyres should not be changing, since that will affect tyre pressure and rolling resistance. All of it cannot be done without a modification to the vehicle suspension and a special wind tunnel setup. In this investigation the following modifications were used. Firstly, the drive-shafts were disconnected and the brake pads removed, therefore eliminating losses associated with them. Secondly, the shock absorbers were replaced by threaded rods, this allowed having the wheels fixed in their positions inside the wheelhouses, see Figure 12.

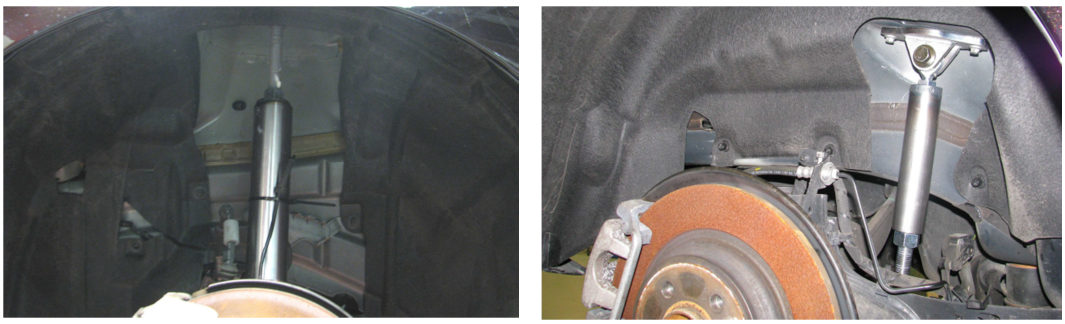

Figure 12. Modified suspension

Fixed suspension allowed to completely support the vehicle by using underbody struts with the wheels secured in their correct driving positions. The contact between the wheels and WDUs was minimised to decrease the rolling resistance moment and to prevent heating of the tyres as much as it was possible. During the velocity sweep the ride height of the vehicle was constantly adjusted in order to compensate for the tyre radial expansion and maintain rolling low resistance. Frictional resistance moment in bearings was estimated using dynamometric screwdriver and assumed to have a constant value. More about the setup can be found in Paper I.

Since all of the losses were either eliminated or estimated, it was possible to measure the part of traction force (F'_{trac}) responsible for overcoming the ventilation resistance moment. This force can be used to calculate the moment itself and hence to get equivalent force (F_{vent}) and consequently ventilation drag coefficient ($C_{D(vent)}$).

The ventilation resistance moment (M_{vent}) can be calculated using equation 2.1, where r' is current wheel centre height that depends on vehicle velocity, see Figure 13:

$$M_{vent}(V) = F'_{trac}(V) \cdot r'(V) \tag{2.1}$$

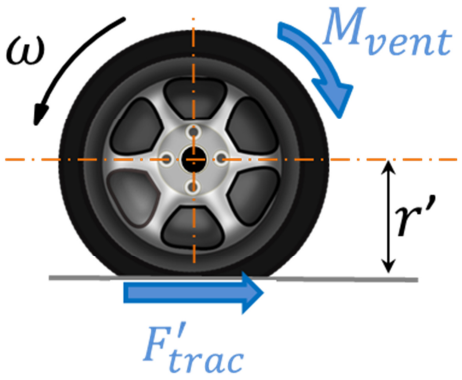

Figure 13. Ventilation resistance measurement

The equivalent ventilation force can be introduced using power required to overcome the moment, this power can be written in two different ways, either using the moment:

$$P_{vent}(V) = M_{vent}(V) \cdot \omega(V) \tag{2.2}$$

or using the equivalent force:

$$P_{vent}(V) = F_{vent}(V) \cdot V \tag{2.3}$$

This power should be the same, therefore:

$$F_{vent}(V) \cdot V = P_{vent}(V) = M_{vent}(V) \cdot \omega(V) \tag{2.4}$$

And by using equation 2.1:

$$F_{vent}(V) \cdot V = F'_{trac}(V) \cdot r'(V) \cdot \omega(V) \tag{2.5}$$

$$F_{vent} = F'_{trac} \tag{2.6}$$

The equivalent ventilation resistance force is equal to the part of the traction force responsible for the ventilation resistance moment, therefore by using equation 1.6 ventilation drag coefficient can be obtained as

$$C_{D(vent)} = \frac{F'_{trac}}{\frac{1}{2}\rho V_{rel}^2 A} \tag{2.7}$$

The setup described was used for measuring and comparing the aerodynamic drag and ventilation resistance moment of different wheel rim designs. For this purpose a set of previously developed five-spoke modular wheels was used [54]. This allowed changing rim configurations without dismounting the wheel, not only making these changes fast but also minimising possible errors associated with the wheel changes during the experiment. All tested rim designs can be found in Figure 14.

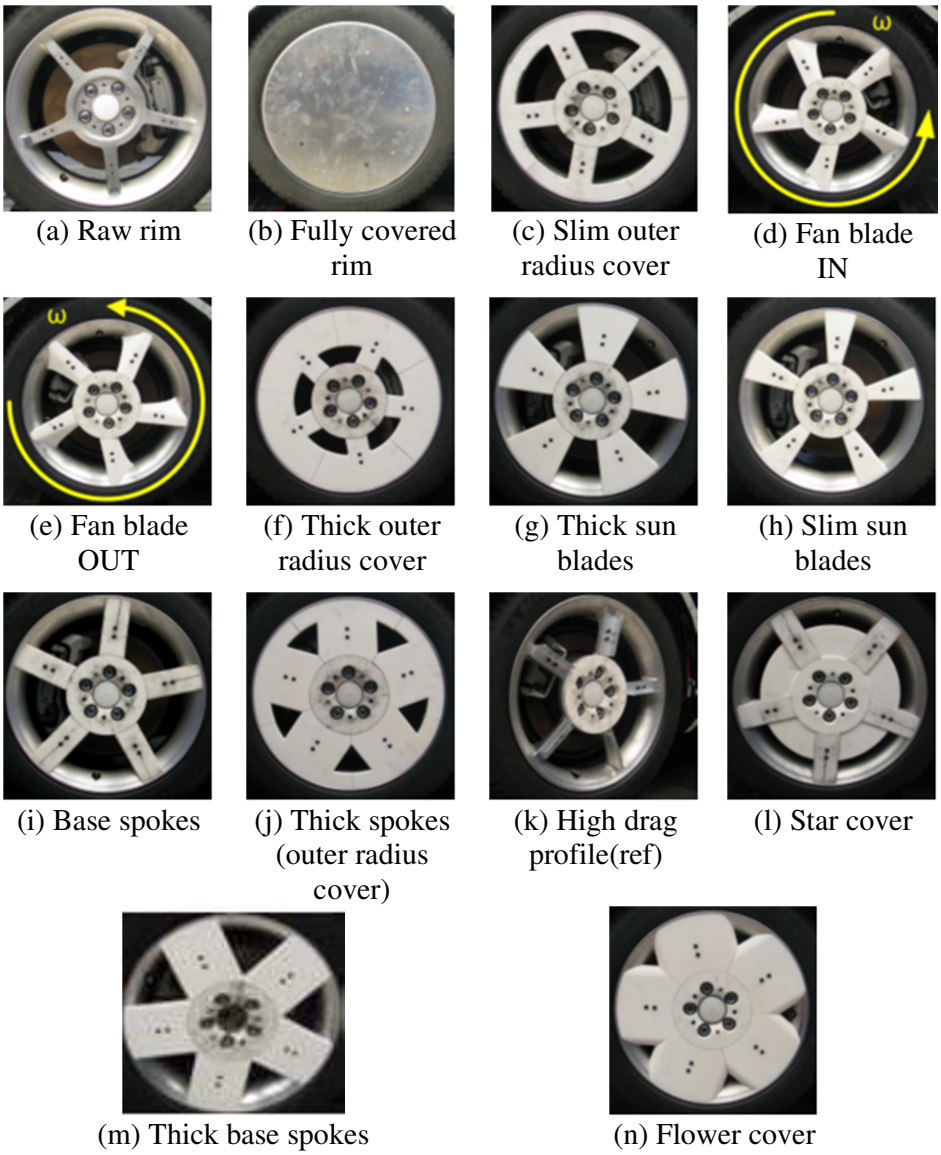

(a) Raw rim (b) Fully covered rim (c) Slim outer radius cover (d) Fan blade IN

(e) Fan blade OUT (f) Thick outer radius cover (g) Thick sun blades (h) Slim sun blades

(i) Base spokes (j) Thick spokes (outer radius cover) (k) High drag profile(ref) (l) Star cover

(m) Thick base spokes (n) Flower cover

Figure 14. Rim designs tested

2.2.2 Tyre deformations and the dependency on vehicle struts used

It is well known that the tyre shape depends on the vehicle speed, since the inertial forces acting on the tyre tend to expand it in radial direction and at the same time compress in axial [36, 35]. As a consequence of radial expansion the wheel centre is lifted, and hence the vehicle ride height will change [55].

In the wind tunnel the vehicle body is usually rigidly connected to the balance and fixed at certain positions measured based on the possible load distributions. This position can be altered, but is usually kept constant during the velocity sweeps. Fixed struts allow to greatly reduce the vertical load on the WDUs, since the struts are supporting a large portion of the vehicle weight, and therefore they are good for durability of the WDU belts.

In order to get a more realistic representation of an on-road vehicle ride height and pitch angle change at different velocities, floating struts can be used, see Figure 15. This type of strut prevents the vehicle from moving in lateral and longitudinal directions, at the same time allowing vertical movement. The obvious drawbacks of using the floating struts are that the vehicle must be initially loaded with weights to get to the desired initial ride height and, most importantly, the vertical forces acting on the WDUs are much higher, since the entire vehicle weight is supported by them.

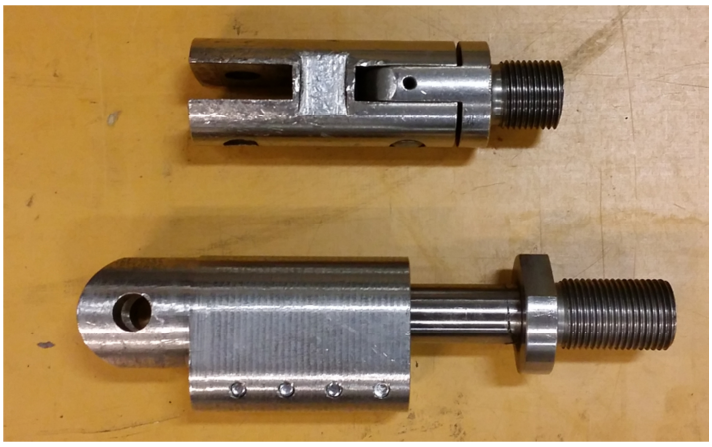

Figure 15. Comparison of fixed(top) and floating(bottom) struts

One of the investigations conducted and discussed in this thesis included comparing the usage of fixed and floating struts with a focus on the differences in tyre shapes, wheel positions and the position of the vehicle body. All of these differences result in alterations in the aerodynamic forces measured.

For the investigation, the vehicle was tested with different struts in the velocities from 0 to 240 km/h. To capture the tyre deformations the wheels were filmed from different angles; and to measure the changes happening to the vehicle body a set of laser displacement transducers was used. The displacements were measured for front and rear suspension arms and, when using floating struts, for the struts movement, see Figure 16. Later based on these displacement measurements the wheel centre height changes and the vehicle body movements were calculated.

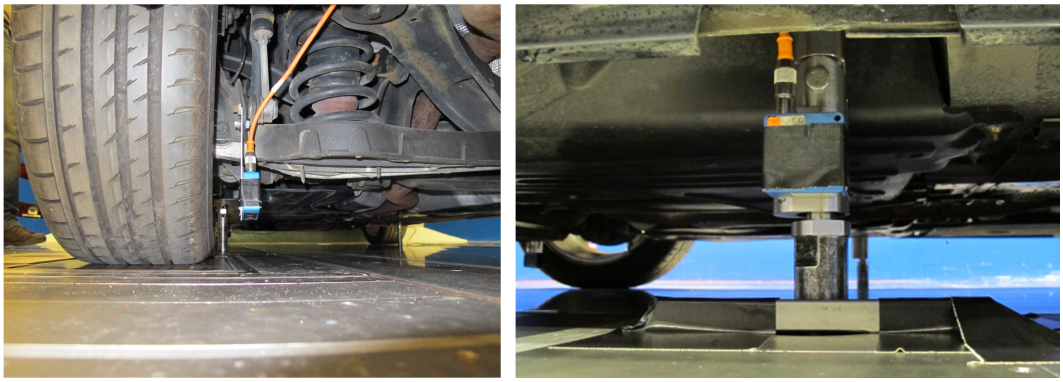

Figure 16. Examples of displacement transducer installation

The tests were conducted with and without the airflow to separate the effects of the body lift due to tyre deformations and the ones due to the aerodynamic lift. Additional test

configurations included covering the frontal cooling inlets, as seen in Figure 17, in order to investigate the effects of different struts on the cooling drag.

Figure 17. Overview of the test setup and covered cooling flow inlets

2.2.3 Combining aerodynamics and thermal management

As a part of the project focused on combining aerodynamics and thermal management for better prediction of brake system performance, another experimental investigation has been conducted. In this test an Alpine descent brake cooling test was replicated in the Volvo wind tunnel. Regular Alpine descent test involves taking the vehicle to a test track in the Alps and driving downhill with more or less constantly engaged brakes. This part of the test is called the heat-up phase. For the second and last phase the vehicle is standing still and the brakes are cooling down; consequently this phase is usually called cool-down or soaking phase. Temperatures of different parts of the brake system are usually monitored and recorded for the entire test and used later for the assessment of brakes system performance.

Due to various reasons, it is not always possible to bring every vehicle to the Alps; therefore a number of different methods were developed to simulate this test locally. As an option a test vehicle can be pushed by an additional vehicle on a flat test track or one can use a chassis dyno or a wind tunnel to simulate the on-road conditions both in terms of braking force and airflow. All of these replication methods require a working vehicle or a prototype to be utilised. Imitation of the brake cooling performance test using numerical simulation methods may allow to perform a virtual test way before a working prototype is ready. As part of the investigation focused on the process development of such simulation method the wind tunnel test was conducted. During this test both heat-up and cool-down phases were performed and the temperature history was recorded for a large number of the brake system parts. Later these temperatures were used in the setup process of the simulation model and for comparison of the results.

Since a significant amount of torque had to be supplied to the front wheels, the vehicle was positioned on a dynamometer which located downstream the moving ground system in the test section. Different parts of ground simulation systems were used to decrease the thickness of the boundary layer. For this test the front right wheelhouse was equipped

with around 150 thermocouples measuring the surface temperatures of different parts as well as the air temperatures around them, see Figure 18 for a general setup of the test. Eight thermocouples were installed inside the brake disk and a slip ring connector was used to obtain the temperature gradients on different sides and different radii of the disk, see Figure 19.

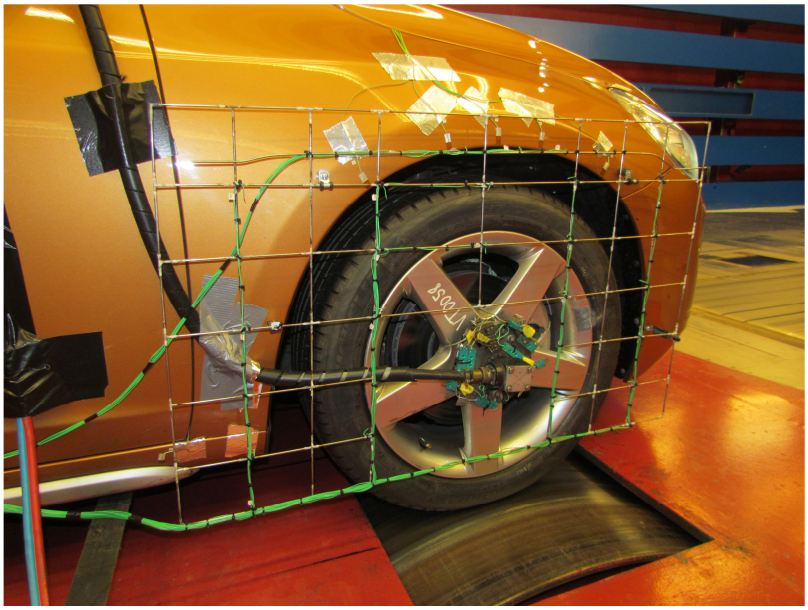

Figure 18. Brake cooling test setup

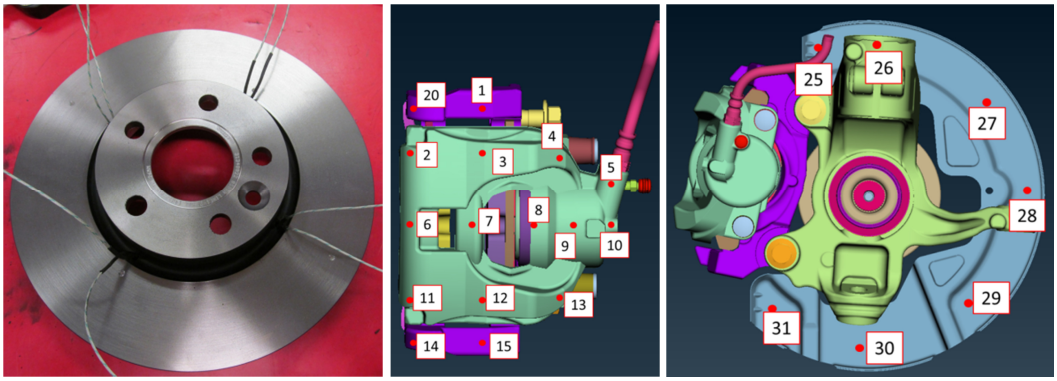

Figure 19. Brake disk equipped with thermocouples and an example of other thermocouples positons

The main temperature that was monitored was a temperature of the brake fluid since it is absolutely crucial for this fluid not to achieve boiling temperature. To achieve the worst case scenario the brake pads were in contact with brakes during the entire experiment, including the cool-down phase. The cases tested included scenarios of running cooling fans and switching them off for the soaking part of the test that has been achieved by installing a control box for the cooling fans, enabling manual rpm adjustment.

To measure the temperatures of tyres and rims, infrared thermometer and thermal camera were utilised. More about the experimental setup can be found in Paper IV.

2.3. Numerical investigations

Numerical simulations performed were conducted in several different commercial CFD software products. Figure 20 shows and overview of a typical CFD procedure. The pre-processing step typically includes obtaining the CAD models of different parts, assembling it together, removing the features that are irrelevant for the simulation often by wrapping of overcomplicated parts, CAD geometry cleaning and initial surface meshing, and lastly grouping parts for easier meshing and solving setup. The meshing step mainly includes the creation of the virtual wind tunnel and dividing it into millions of volumetric cells that is later supplied to a solver to perform the simulation. Lastly the results are post-processed and the values needed are obtained.

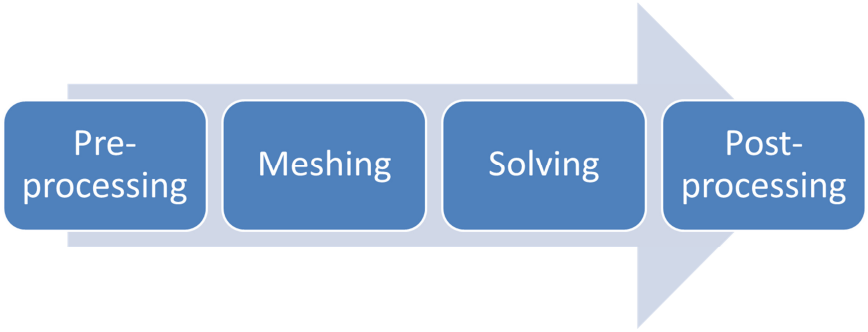

Figure 20. Standard CFD procedure

2.3.1 Numerical setups used

The pre-processing step was always conducted in ANSA software supplied by BETA CAE Systems S.A [56], an example of the resulting geometry can be seen in Figure 21. In addition to typical steps a number of construction surfaces were added to the model in this step to separate the areas of different mesh type or regions with different physics specified, for example sliding mesh, Multiple Reference Frame regions for wheel spokes or sliding mesh regions in Paper V. For Paper IV a highly detailed representation of the brake system was also added to the CAD model, see Figure 21.

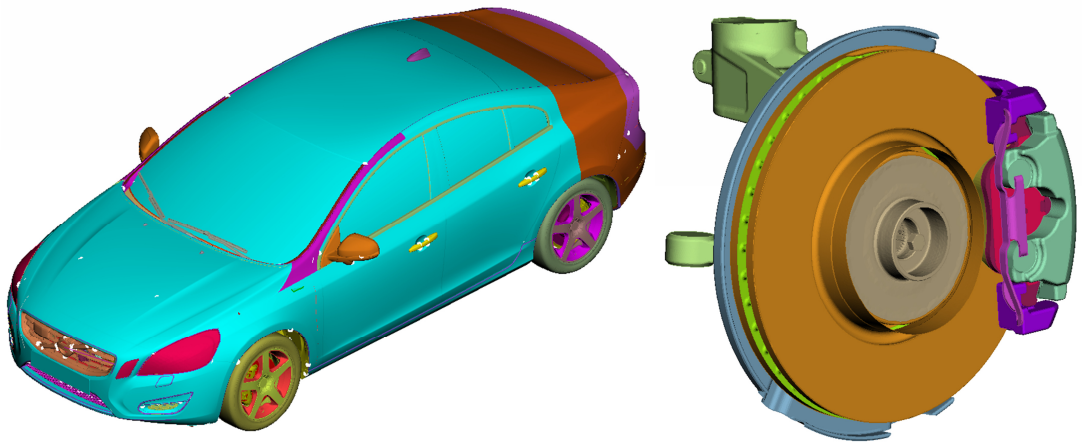

Figure 21. Main CAD model of the Volvo S60 vehicle and a brake system used in Paper IV

The rest of the procedure after the pre-processing step was not the same for different investigations due to the different software products used. The investigations for Paper II

and Paper III were conducted using STAR-CCM+ software produced by CD-adapco [57]. This software was used for volume meshing, solving and post-processing. The surface meshing in Paper IV was done using ANSA-Tgrid method and for the volume mesh Fluent Mesher was used [58, 59]; for Paper V volume meshing was performed in ANSA and Harpoon software [60]. The solving in Paper IV and Paper V was performed in ANSYS Fluent and the post-processing in EnSight by CEI Software [61].

For the Meshing step the model was put in a virtual simplified idealized wind tunnel. This tunnel is essentially just a box that is large enough not to produce any significant blockage effects. The wind tunnel volume was meshed with multiple refinement areas added around the vehicle and behind it, see Figure 22. Typical final volume mesh was between 80 and 120 million cells. Since Paper IV included thermal conduction inside the material of different brake system parts, these parts had to me meshed as well, see Figure 22. The meshing was performed in accordance with recommendations with internal Volvo automotive CFD procedure as well as the recommendations obtained from software manufacturers [62, 63, 64]. The same recommendations were used in the solving step.

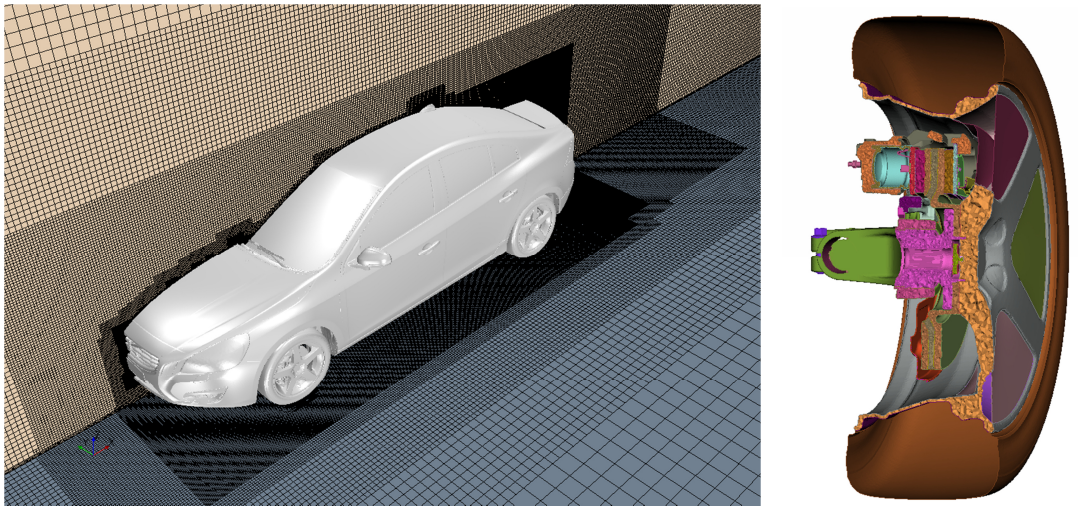

Figure 22. Examples of fluid and solid volume mesh

For the solving step the boundary conditions applied included moving wall for the entire wind tunnel ground and symmetry conditions for all walls. The inlet air velocity was used to assign not only the velocity of the moving ground but also to calculate the rotational velocities of the wheels and cooling system fans.

Most of the simulations conducted for the investigations were done in steady state mode using Reynolds Averaged Navier Stokes (RANS) equations. The only exception was Paper V where some unsteady RANS simulations were conducted due to the usage of the sliding mesh approach. The realisable k-ε turbulence model was selected for all investigations as it is known to be robust and to produce satisfactory results at relatively low computational costs [62, 63, 65, 66]. More sophisticated simulation models such as Large Eddy Simulation (LES) or Detached Eddy Simulation (DES) were not considered in this thesis due to their extremely high computational costs especially when using fully detailed vehicle geometry.

Prismatic layers were used on all of the vehicle surfaces in order to ensure y+ values in an acceptable range for the near wall modelling. The wheels and fans rotation was in most cases modelled using rotating wall boundary condition and Multiple Reference Frame(MRF) method, the only exception was Paper V, where the sliding mesh approach was tested. In case if the cooling package was simulated in the investigation, it was handled by using porous media model. More about numerical setups can be found in relevant papers appended.

2.3.2 Wheel modelling and rotation

It is known that the tyre shape alters with changing speed of the vehicle; hence if different velocities are to be modelled in the numerical simulation, the wheel surfaces need to be morphed. This morphing is usually done using 4 parameters: 3 wheel deformations introduced before (axial compression, radial expansion and wheel centre lift) and a tyre bulge; the last one here is responsible for the change of tyre shape next to the contact patch [36]. The standard tyres that are usually used for CFD simulations are simplified (slick), they do not have any tyre treads, nevertheless they have a correct general shape, obtained based on the tyre manufacturer's data and wind tunnel observations. As a part of Paper III the experimental test with changing ride height and changing tyre shape was simulated in CFD. The wheels were morphed to correspond to the shapes observed in the wind tunnel. For the simulation of floating struts case, the vehicle body was lifted and rotated to capture the changing ride height and pitch angle.

It is known that the presence of tyre pattern affects the airflow around the wheelhouses and consequently has an effect on aerodynamic drag and lift [37, 38]. Paper V looks into the effects that the addition of the tyre patterns has on the aerodynamic resistance moment calculated using CFD. Three different tyre patterns investigated can be seen in Figure 23.

Tyre A(Slick tyre) *Tyre B* *Tyre C*

Figure 23. Tyre patterns compared

Another topic investigated in Paper V is different rotation simulation techniques for the tyres. Traditionally the wheel spokes rotation is modelled by an addition of MRF region for the spokes. Even though the rim is standing still in this case, this method works well because the MRF application allows to capture the pressure distribution on the wheel rim and impose correct velocities to the surfaces inside the region. The tyre rotation is usually simulated by the application of a moving wall boundary condition. This works well for slick tyres, but results in a problem for tyres with grooves, since this type of boundary condition only allows setting the velocity tangential to the surface. Similarly to the rims, MRF approach can be applied to the air inside tyre treads.

Paper V investigated different methods of rotation simulation for tyres with pattern and their effects on the ventilation resistance moment. Standard rotating wall boundary

condition is compared to the application of MRF approach. Two options are investigated: application of the MRF in the first cell all around the tyre and only applying it to the first volumetric cell inside the grooves, see Figure 24. The last option will be referend to as MRFG method [38].

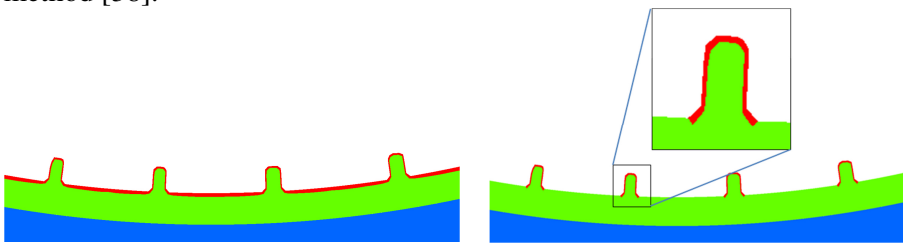

Figure 24. MRF regions for the diggerent methods: MRF(left) and MRFG(right)

These three steady-state methods are compared to a sliding mesh approach where the wheels are enclosed in their own isolated volumes which physically rotate, see Figure 25. Such an approach usually allows getting a more accurate time-dependant solution, but at the same time it is much more computationally expensive. Additionally, since the entire wheel geometry is actually rotating, it is impossible to have any contact patch deformation. Moreover, as there is a rotating volume mesh region around the wheel, the tyre cannot be positioned in contact with the ground at all, leaving a small gap and resulting in a "flying" vehicle case.

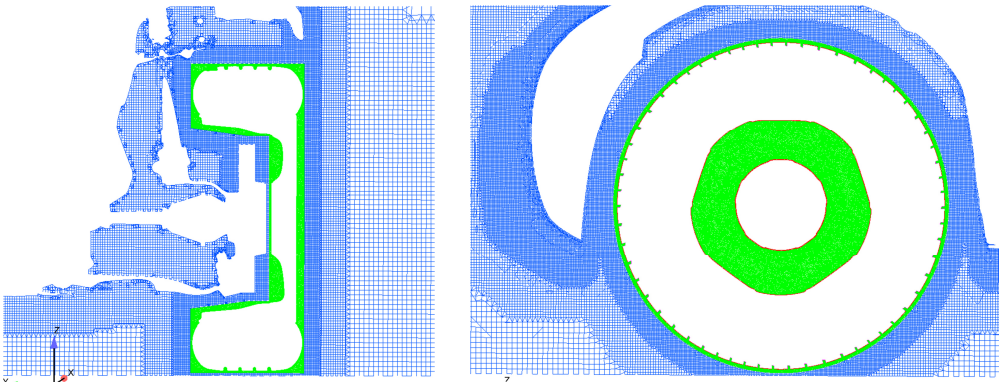

Figure 25. Cross-section cuts through the sliding mesh volume around the wheel

2.3.3 Cool-down simulation

Most often when adding thermal management to aerodynamic investigations a second thermal solver is used; this requires coupling of two software products. In case of the investigation presented in Paper IV both aerodynamic and thermal calculation were performed inside ANSYS Fluent.

As discussed previously, Alpine descent test consists of two phases: heat-up and cool-down. These phases are significantly different from the computational perspective. During the heat-up the vehicle is moving and the wheels are rotating, moreover there is an energy input to the system from the contact between the brake disk and pads. For the second phase the vehicle is standing still with no additional heat generation. Paper IV summarises the first step in the process development project and only includes the cool-down stage simulation. The heat-up stage will be simulated in the continuation of the project.

Since the vehicle is standing, there is no need to use MRF or sliding mesh. The wheel is set in the same position as during the experiment and a number of monitoring points added to different parts to record the temperature history as the parts cool. Even though the brake system is modelled with a high level of detail, the rest of the model is significantly simplified in order to decrease the computational cost of the simulation. For example, the engine bay was completely sealed, considerably reducing the volumetric cell count, see Figure 26.

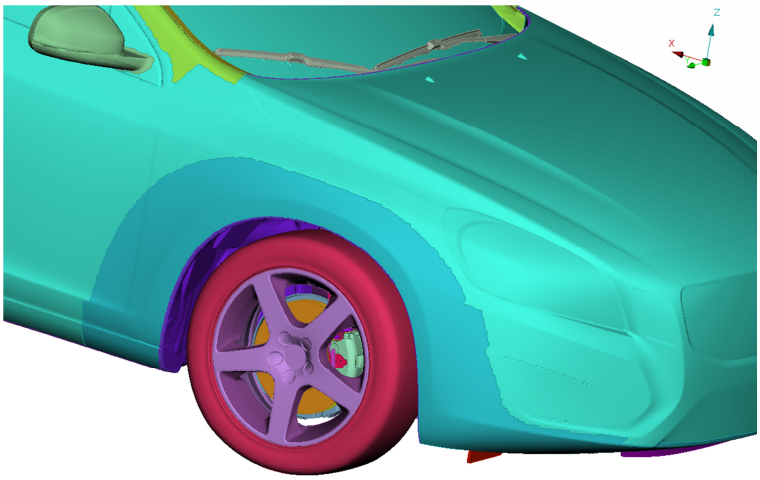

Figure 26. Model of a cool-down simulation with sealed engine bay

The temperatures of the parts are changing significantly slower compared to changes happening to the airflow, moreover to decrease the computational cost and to simplify the procedure, it is possible to use steady-state simulations to obtain just a mean airflow picture at certain time intervals, therefore creating a multiple steps procedure. Firstly, the part temperatures are assigned based on the values measured in the wind tunnel and a convection-driven airflow is computed. Secondly, the airflow is frozen and the temperatures of the parts are allowed to change. After a while the airflow is recalculated and the cycle continues. Since the process is under development, it has a number of limitations, most of which are addressed in Paper IV.

3. Summary of the results

This chapter contains a summary of the most important findings of the research project. Full descriptions of the results and more discussions can be found in the appended papers.

3.1. Wheel deformation and ride height change

As discussed in chapter 2, the tyre deformations were filmed from different angles to obtain the shape dependency on the vehicle velocity and also to compare the differences between fixed and floating struts setups. Figure 27 shows instantaneous frames from the video footage comparing tyre shapes for two different velocities: 0 and 240 km/h. The example is given for the floating strut, the vertical movement of which can be easily observed.

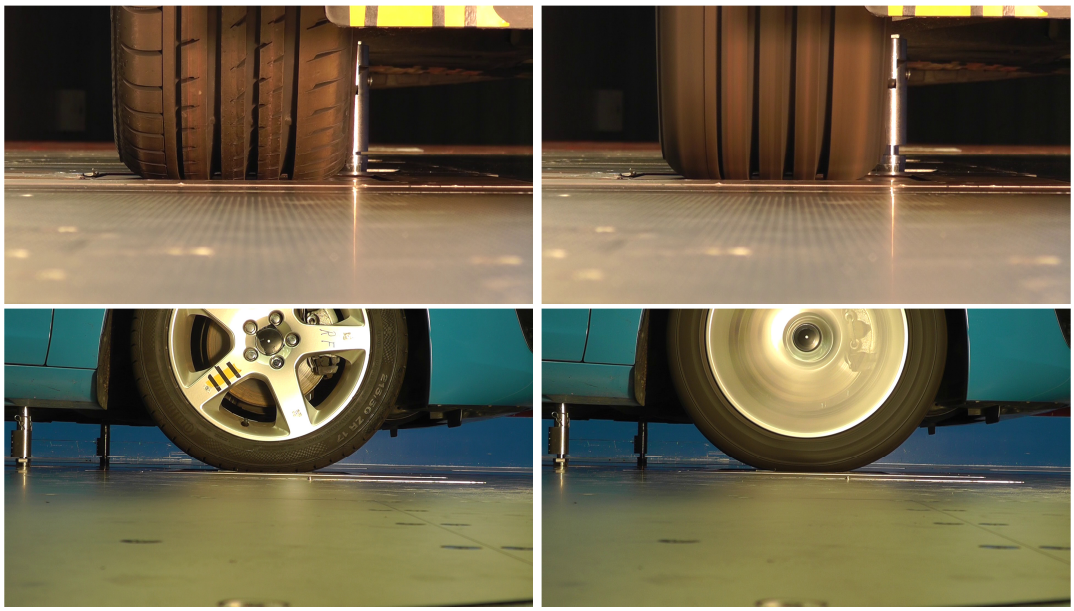

Figure 27. Tyre shape comparison for 0 and 240 km/h; floating struts case

By analysing the videos obtained with fixed and floating struts it was found that radial expansion and axial compression of the tyres were almost identical for these two cases. See Figure 28 for an example of deformations measured for the front right wheel. It can be observed that both radial expansion and axial compression show quadratic relationship, as previously suggested by other authors [36].

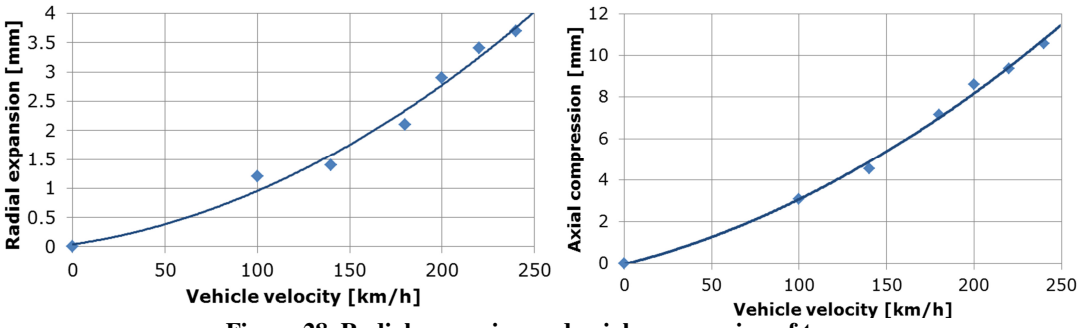

Figure 28. Radial expansion and axial compression of tyres

The main difference in tyre deformations between two cases was observed in the wheel centre lift, see Figure 29 for the comparison for the front wheels. It can be seen that the vertical displacement of wheel centre is higher for the case of floating strut. The two main reasons for that are:

- lower initial wheel centre height for the floating struts due to higher weight supported by the wheels;
- changing ride height of the vehicle, that allows to keep vehicle suspension in more or less the same position.

In case of fixed struts changing wheel position inside the wheelhouse leads to increased load on the suspension springs and therefore higher vertical load on the wheel.

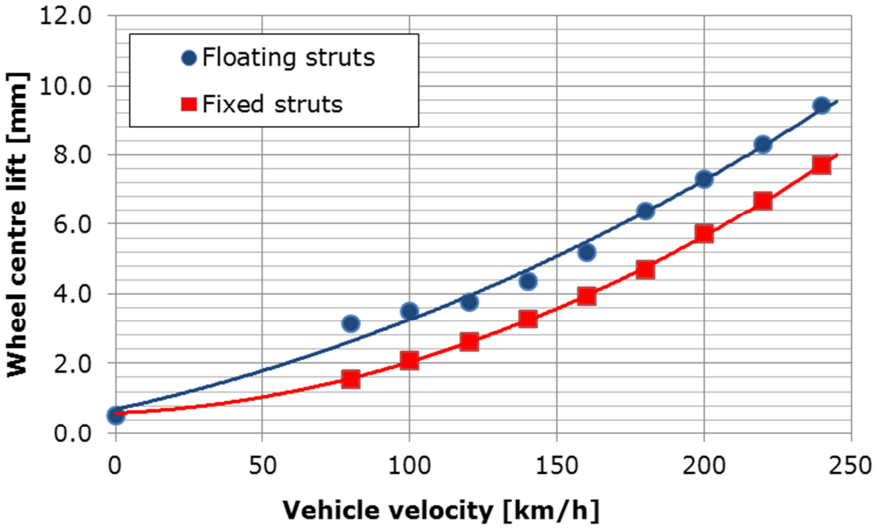

Figure 29. Wheel centre height changing with speed

Initial positive displacement that is present in Figure 29 and that will be observed for the body displacements graphs in Figure 30 is the residual deformations in the tyres due to temperature effects. Since the there were multiple tests conducted one after another, there was not enough time for tyres to return to the room temperature and, therefore, the these deformations were measured. The maximum residual wheel centre lift was observed when the vehicle went from top speed to zero and it was about 2 mm. This effect can be an important factor to consider when conducting multiple tests without much time between them.

Figure 30 shows the front and rear axle displacements for different investigations with floating struts. By comparing wind on and wind off scenarios, it is possible to separate the effects of the aerodynamic lift force and wheel rotation. It can be seen that with just wheel rotation and no aerodynamic load the lift of front and rear of the vehicle is almost the same. On the other hand, in case of wind on there is a significant difference between front and rear. This means that not only the vehicle ride height is changing, but also the pitch angle of the vehicle. It can be seen that the rear body lift can be as high as 17 mm for the case of 240 km/h.

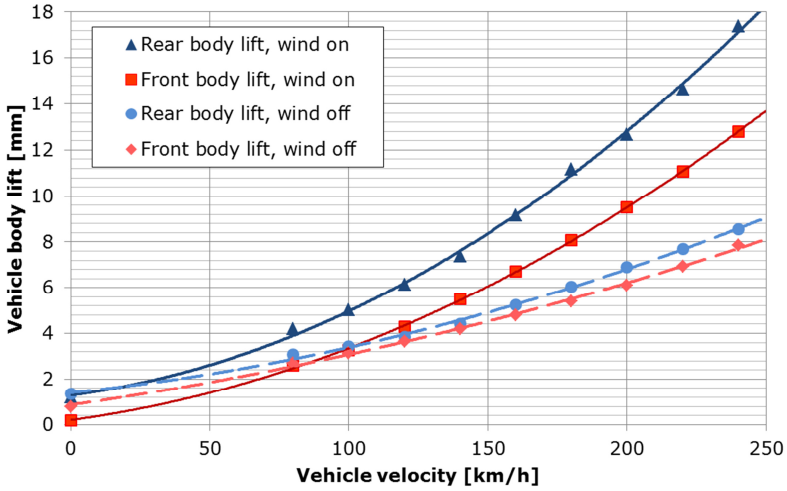

Figure 30. Vehicle body displacements in relation to vehicle velocity

All of these vehicle displacements and tyre deformations lead to the difference in vehicle geometry and position, hence resulting in the changing aerodynamic drag coefficient. The C_D was measured in the wind tunnel and was calculated using numerical CFD simulations, where the vehicle geometry was modified to correspond to the changes observed during the experiment. The resulting graphs can be found in Figure 31 where the values are given in relation to the 80 km/h case with fixed struts.

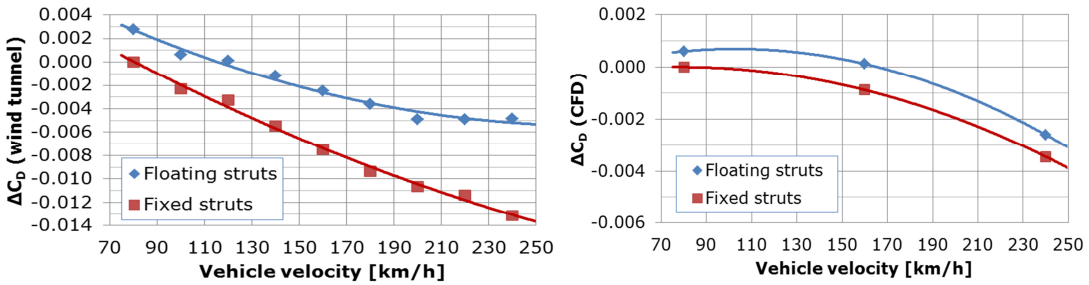

Figure 31. Drag coefficient behaviour in relation to velocity for wind tunnel tests and CFD simulations

It can be seen that the aerodynamic drag coefficient is decreasing with speed for both cases, but the gradient is gentler in the case of floating struts. This behaviour has already been observed for the case of fixed struts, and it is probably a result of a reduced distance between the tyre and wheelhouse in radial direction [35, 67, 68]. This could also explain the difference in behaviour between fixed and floating strut cases, since the wheel position inside the wheelhouse is different in these cases, with larger gaps in case of floating struts. It should be pointed out that there may be changes to the vehicle geometry that happen with increased velocity and that were not measured during the experiment; for example increasing gaps between other parts or flexing of thin panels and flaps. These small changes can easily have an effect on the aerodynamic drag of the vehicle.

Another observation that can be made from comparing drag curves is that the aerodynamic drag measured with floating struts was always higher. The difference was as high as 8 drag counts at high velocities, but it was also present at low velocities. The reason for that may be in the fact that even though starting from the same initial position in terms of front and rear body height, by reaching 80 km/h the ride height of the vehicle mounted on floating struts was already changed by about 4 mm, see Figure 30.

CFD results are showing the same decreasing trend and also capturing the fact that the use of floating struts is resulting in slightly higher aerodynamic drag coefficient. However, the magnitude of changes captured was less significant, which was probably caused by the number of simplifications that were used in the numerical setup.

The changes in vehicle position also resulted in differences in measured cooling drag of the vehicle. The cooling drag is usually defined as a difference in aerodynamic drag force for the vehicle with open and closed front air inlets on the grill. Figure 32 shows the cooling drag values derived from the wind tunnel tests data. It can be seen that in case of floating struts the cooling drag was always higher with a difference reaching 4 drag counts.

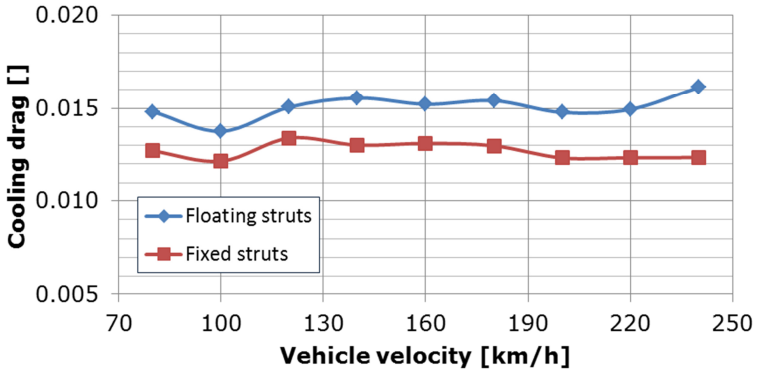

Figure 32. Cooling drag for cases of different struts

More discussions about the results including the differences introduced to aerodynamic lift force distribution can be found in Paper III.

3.2. Aerodynamic resistance moment

3.2.1 Experiments

Using the setup described in section 2.2 the power required to overcome the aerodynamic resistance moment of the wheel was measured, see Figure 33. It can be seen that at top speed the difference between the worst and the best design was around 30%, refer Figure 14 for the images of all designs tested. The worst performing rim design (high drag wings) was used as a reference for all other comparisons.

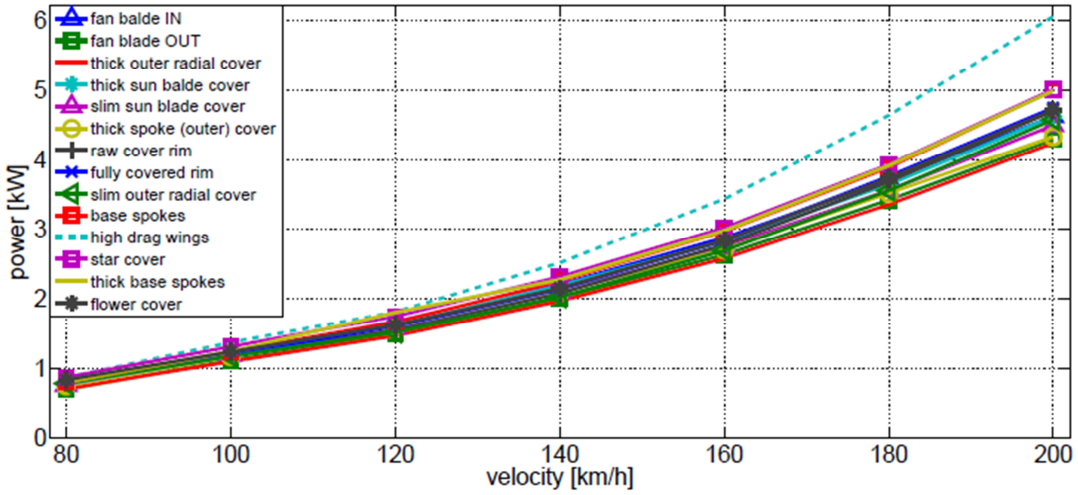

Figure 33. Power requirement for four wheels in reference to the rim designs tested

These power curves can be recalculated to equivalent ventilation drag force and to ventilation drag coefficient, according to equations presented in section 2.2.1. Figure 34 compares 5 different rim designs, the results are presented in terms of percentage difference in comparison to the high drag wings rim results. The results for other rims can be found in Paper I. The rim with covered outer radius and the one with aerodynamically shaped spokes are performing better compared to other designs presented. Fully covered rim that does not allow any flow through the wheel are the third best.

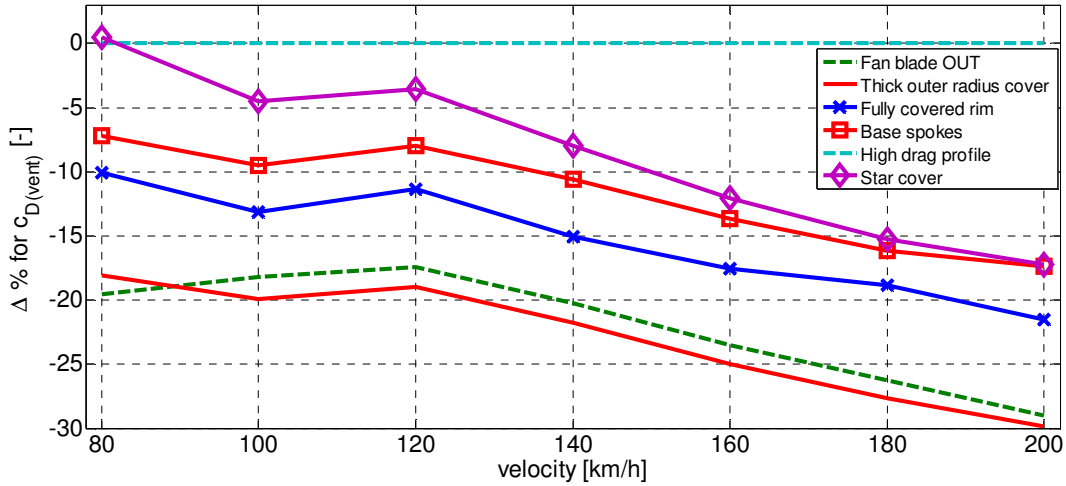

Figure 34. Ventilation resistance coefficient comparison for different rim configurations

It is well known that, changing the rim of the wheel has a significant effect on the aerodynamic drag of the vehicle [34], therefore it has to be taken into account. See Figure 35 for a comparison of aerodynamic drag coefficients, calculated using the force balance. Predictably, the fully covered wheel rims as well as the wheels with significant coverage of outer radius resulted in a lower aerodynamic drag coefficient compared to other designs [54, 33]. It should be noted that even though percentagewise the effects of changing the rims is lower for the aerodynamic drag coefficient of the vehicle the absolute difference is lower for the ventilation drag coefficient.

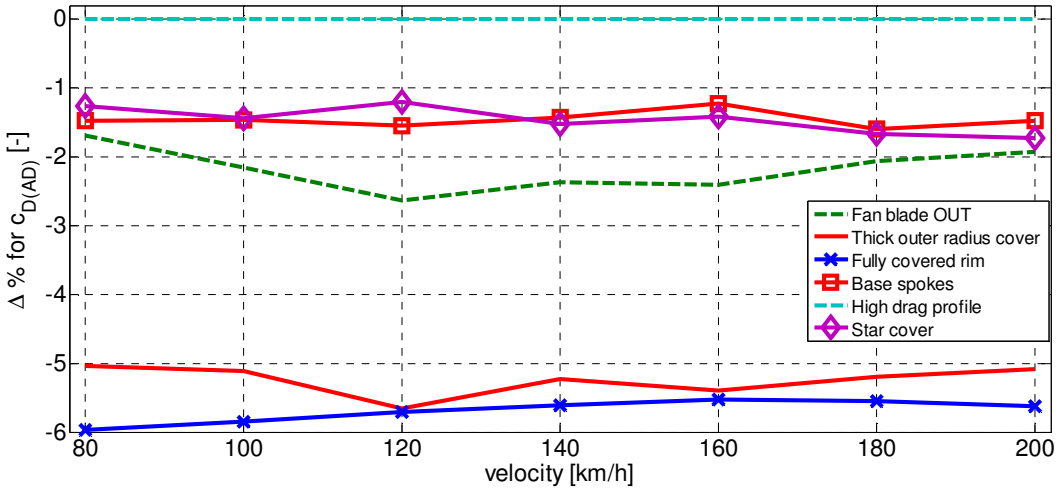

Figure 35. Aerodynamic resistance coefficient comparison for different rim configurations

Due to the way the equivalent ventilation drag force is introduced (equation 1.4), the effects of aerodynamic drag force and the ventilation resistance moment can be combined and used in the driving resistance equation as one total aerodynamic resistance:

$$F'_D = \frac{1}{2}\left(C_{D(AD)} + C_{D(vent)}\right)A\rho V_{rel}^2 \tag{3.1}$$

or

$$F'_D = \frac{1}{2}C_{D(Tot)}A\rho V_{rel}^2 \tag{3.2}$$

A sum of aerodynamic drag coefficient and ventilation drag coefficient ($C_{D(Tot)}$) is compared for different rim designs in Figure 36. Comparing this figure to Figure 35 the importance of the ventilation resistance moment investigations can be observed. The fully covered rim, that showed best results in terms of aerodynamic drag force, is only in the second best position in terms of total aerodynamic resistance due to its relatively ventilation resistance moment. The best results in this case were shown by thick outer radius rim design, since it had relativity low $C_{D(AD)}$ and $C_{D(vent)}$ compared to other designs.

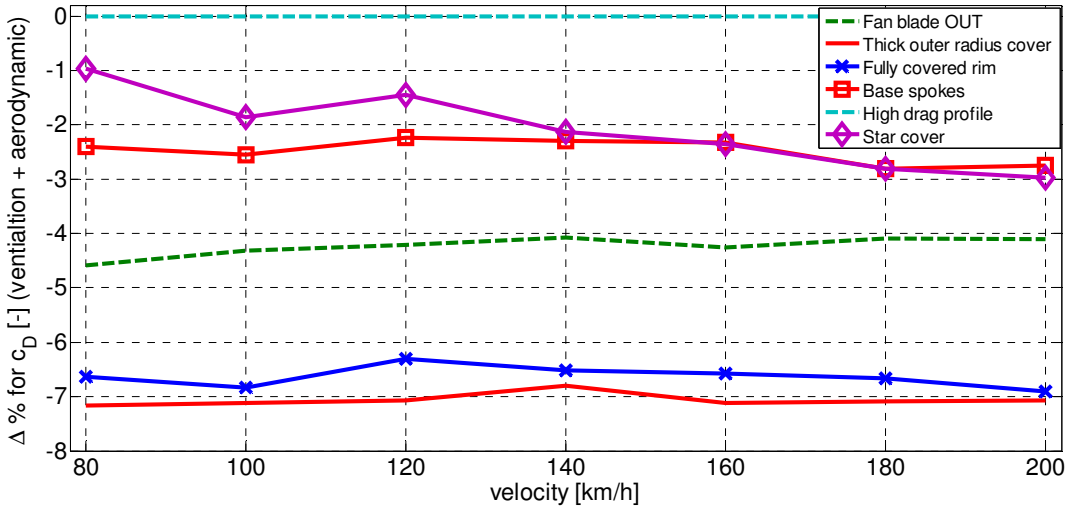

Figure 36. Total aerodynamic resistance comparison for different rim configurations

In general comparing all 14 designs, the wheels with large area covered performed better in terms of aerodynamic drag force and, since $C_{D(AD)}$ is considerably higher than $C_{D(vent)}$, these designs ended up as the best in terms of low total aerodynamic drag coefficient. Nevertheless, since the aerodynamic resistance moment for these rim designs was varying the total drag coefficient was significantly affected by it, altering the order of the best designs.

More wheel rim designs can be created and tested, however there are a number of considerations that should be taken into account:

- A large covered area blocks a considerable amount of the airflow going through the rim, therefore it may have a negative effect on the cooling of brakes;
- A large part of the aerodynamic resistance moment is coming from the tyre, moreover the tyres have significant effect on the aerodynamic drag of the vehicle, hence it can be better to test tyre-rim combinations and not just tyres and just rims;
- Some part of ventilation resistance may be measured during rolling resistance tests and included in the rolling resistance coefficient, thus the equation 1.5 should be applied with caution.

The experimental setup used for this test requires a significant modification to the vehicle suspension. Fixed struts allow lifting the vehicle and getting the tyres barely in contact with the wheel drive units, so there is no realistic tyre deformation in the contact patch area and general tyre shape is different from the one that it would have in real-life scenario. Moreover, since the vehicle is constantly being lifted the vehicle ride height changes therefore affecting aerodynamic drag of the vehicle, as was shown in section 3.1. Nevertheless, the results showed that the measurement of wheel aerodynamic resistance moment is possible and that its effects should not be neglected during the rim design process.

3.2.1 Numerical simulations

A number of simulations were conducted to investigate the ventilation resistance moment and the ways it can be estimated.

The first set of simulations used detailed vehicle model with simplified slick tyres and two different rim designs, see Figure 37. Using the steady-state simulations and MRF regions between spokes to mimic the wheel rotation, the effects of covering the rims on front and rear wheels were investigated.

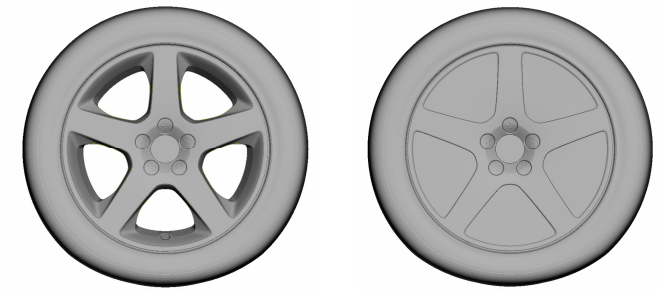

Figure 37. Rim designs investigated: Baseline and Covered

It was shown that it is possible to estimate the effects of changing the rim design on the aerodynamic drag of the vehicle and on the aerodynamic resistance moment. It was found that covering the wheels of one axle the ventilation torque on this axle was significantly reduced, while wheels of the second axle were almost unaffected. The main reason for that being changing pressure distribution on the spokes of the wheel, see Figure 38. This figure shows the pressure coefficient on wheel surfaces for the Baseline and Covered wheels. The cover for the Covered configuration is hidden to show the pressure distribution on the inner surfaces. It can be seen that in the first case the exposed spokes have pressure peaks, which are not there if the wheel cover is introduced.

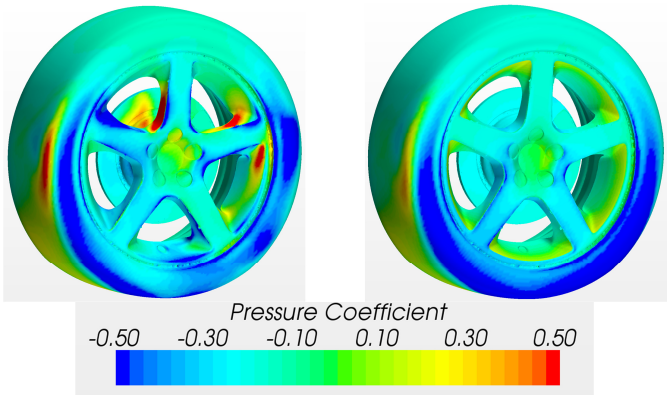

Figure 38. Pressure coefficient on the surface of rear wheel

The effects of wheel covers introduction to front and rear axles in terms of aerodynamic drag counts are presented in Table 1. It was known that working with rear wheels has higher potential in terms of reducing the aerodynamic drag force of the vehicle [69]. Same trend was also observed for the aerodynamic resistance moment. Another interesting observation made was that the forces assessed behave in quasi-independent manner: covering all wheels gives a drag reduction equal to the sum of reductions obtained by just covering front and just covering rear combined. This is valid for both ventilation resistance and aerodynamic drag force.

	Front covered	Rear covered	All Covered
$\Delta C_{D(aero)}$	-3	-10	-13
$\Delta C_{D(vent)}$	-1	-3	-4
$\Delta C_{D(aero+vent)}$	-4	-13	-17

Table 1. Drag counts reduction achieved by covering the wheels

Even though the rims have a big effect on the wheel ventilation moment, it was found that the tyres are responsible for the major part of it. This finding was especially interesting since the tyres in the simulations were simplified and it was already known that the presence of tyre pattern can have significant effect on the airflow around the wheel and on the aerodynamic drag of the vehicle in general [37]. A new set of investigations has been conducted with a focus on tyres and simulation of the wheel rotation.

As described in section 2.3.2, there is a challenge with having tyres with pattern in the numerical simulations. In this investigation 4 different approaches were investigated with 3 different tyres, see Figure 23 for comparison of the tyre patterns. The approaches

included simple rotating wall boundary condition, MRF method applied in the first volume cell around the wheel, MRFG approach with MRF applied only inside tyre grooves, and lastly the sliding mesh approach with a small mesh region containing the wheel actually rotating, see section 2.3.2 and Figure 25.

Figure 39 and Figure 40 shows the aerodynamic resistance moment calculated for one front and one rear wheel respectively. It should be noted that due to the requirements of sliding mesh approach the wheels were positioned with a small distance from the ground and the shape deformation of the wheel in the contact patch region was not modelled. Both of these limitations are resulting in the absolute values that do not correspond to the real life or wind tunnel scenario. Nevertheless, the comparison of 4 methods was still possible and the effects of having a pattern on the tyre were observed.

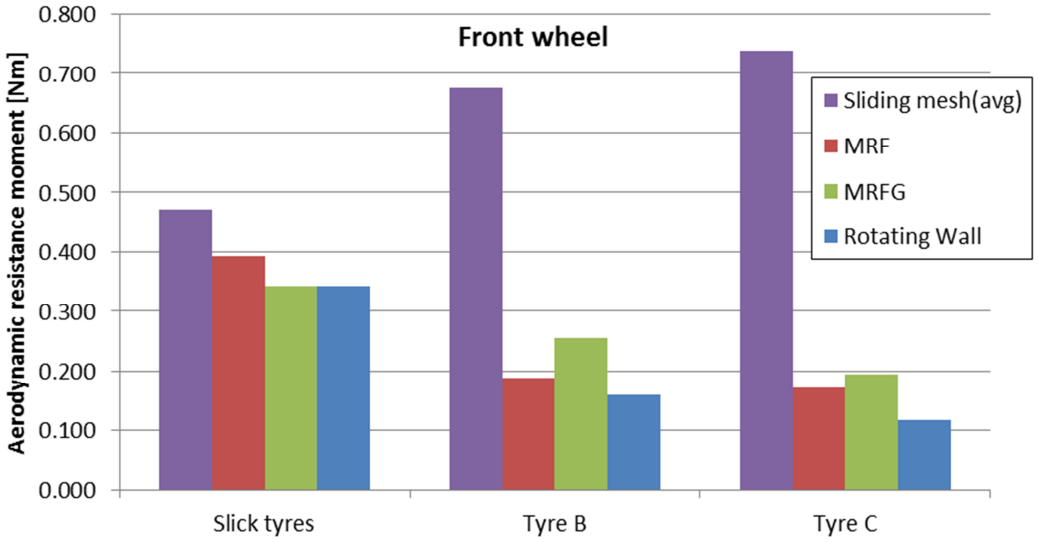

Figure 39. Ventilation resistance moment for one front wheel

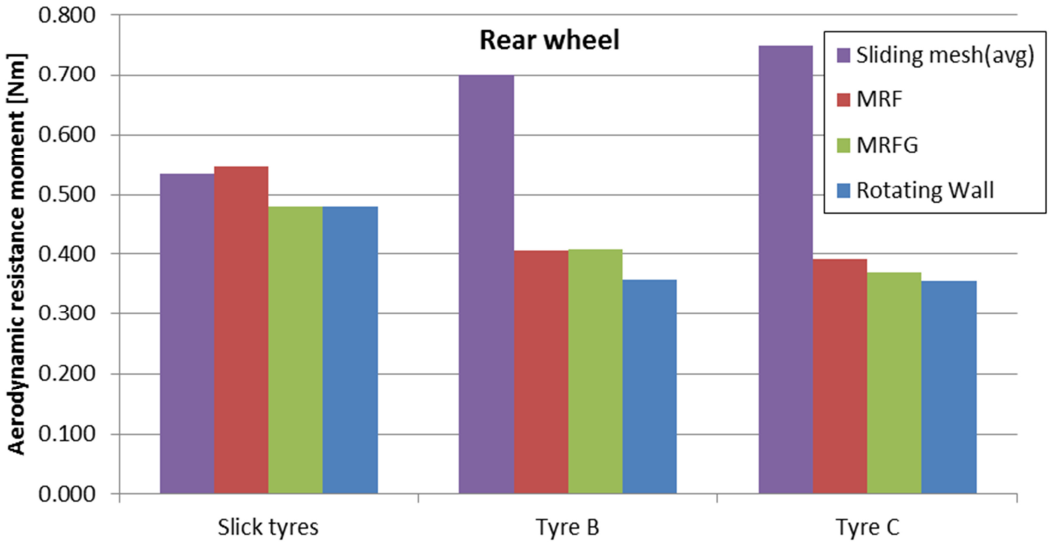

Figure 40. Ventilation resistance moment for one rear wheel

It can be seen that all steady-state approaches are showing a decrease in calculated ventilation resistance moment when the tyre pattern is introduced. It is especially

noticeable for the front wheels that are more exposed to the oncoming air. The results of the sliding mesh approach are exactly the opposite, moreover in some cases the moment calculated can be as much as three times higher compared to the steady-state methods. The only case where the sliding mesh results match with the rest of the approaches tested is the case of slick tyres. The exact reason for such a large difference between sliding mesh and steady-state approaches for tyres with patters requires further investigations.

One part that requires special attention is the brake disk. In both sets of investigations it was set to have a rotating wall boundary condition that resulted in almost negligible resistance moment of its own. Moreover, as can be seen from Figure 25, the sliding mesh volume did not include the brake disk, and therefore the results presented in Figure 39 and Figure 40 did not include the resistance moment of the brake disk. In a separate investigation it was found that the application of rotating wall boundary condition for a ventilated brake disk results in the significant under-prediction of its resistance moment [70]. The results of the sliding mesh and MRF approaches were close, therefore for further steady-state investigations it is recommended to use the MRF approach.

3.3. Brake cooling

3.3.1 Experiments

As discussed in section 2.2.3 two different cases were tested in the wind tunnel: one with keeping the cooling system fans running during the soaking phase and another one with switching them off. Figure 41 shows a comparison of temperatures for the air entering the wheelhouse from the engine bay; left and right wheelhouses are compared. The time scale is shifted in a way that 0 is exactly at the start of soaking phase. Due to the packaging of under hood compartment the right wheelhouse is always warmer than the left one, as long as there is air coming from the engine bay. Since the worst case scenario was to be investigated, the experiment focused on the right side of the vehicle.

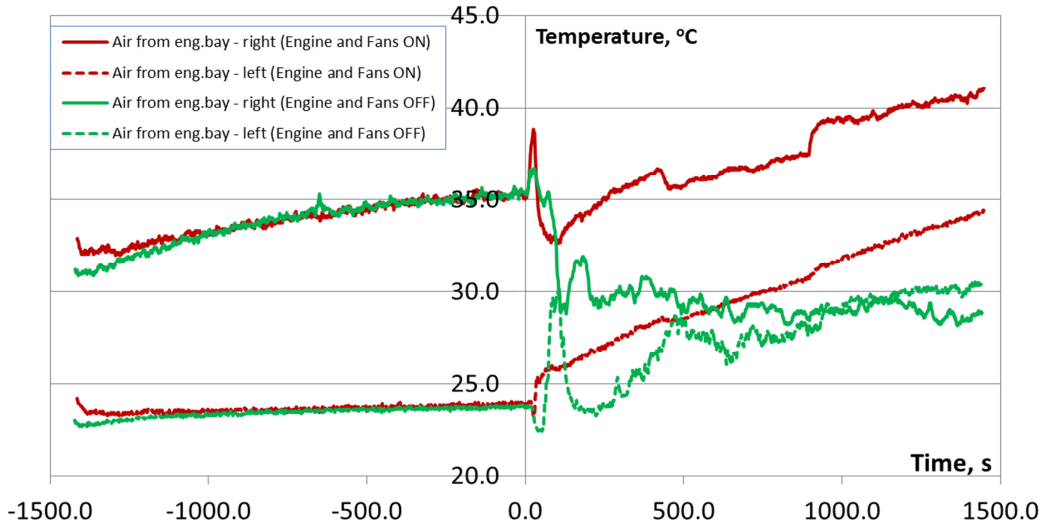

Figure 41. Temperature of the air inside left and right wheelhouses for two cases investigated

The temperature history was collected for all installed thermocouples, allowing the access to temperature gradients and their development over almost 50 minutes time of each test.

This data was used for the initialization of a soaking phase simulation and will be used later for validation of the simulation model when it is ready.

Figure 42 shows the brake fluid temperature changing over time for the two cases. It can be seen that in case of running engine and cooling fans, even though the air temperatures inside the wheelhouse are higher, the brake fluid temperature is lower at every given moment. This behaviour was confirmed by repetition of the tests and can also be seen in the cool-down curves for the other parts. In other words, additional air-flow from the engine bay increases the speed of soaking process. A likely explanation is that, if the fans are running, even though the air temperatures get higher, there is a forced airflow inside the wheelhouse and therefore higher convective heat transfer rate.

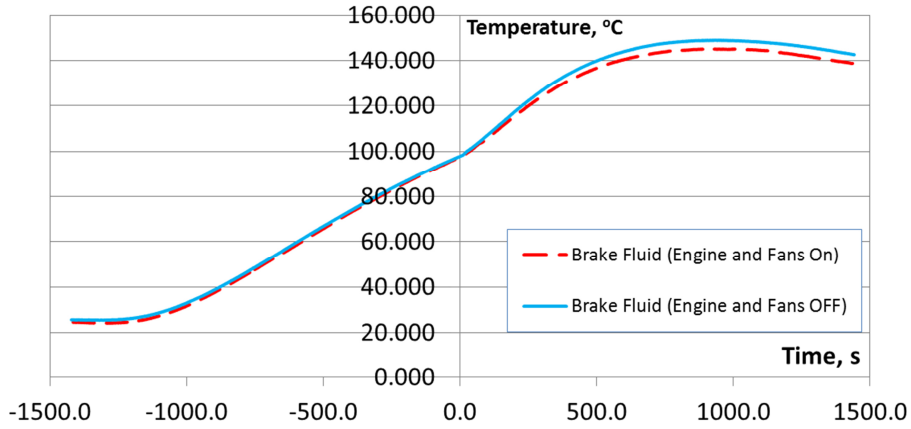

Figure 42. Brake fluid temperature for two cases

An interesting result was observed when looking at the temperature history of a brake disk. The disk was equipped with 8 thermocouples, 4 installed on finger and 4 on piston sides of the disk. The radius on which the temperature was measured was also varying, see Figure 43. The figure also shows the temperature history obtained for different points with "F" and "P" representing finger and piston side respectively. One can see that difference in temperatures between points 1F and 3F during heat-up phase reached around 100°C, even though these points are on the same radii of the same side of the wheel. Such high temperature gradients during the braking process are normal and can be attributed to several reasons; mainly they occur due to multiple hot spots developing on the surface [71].

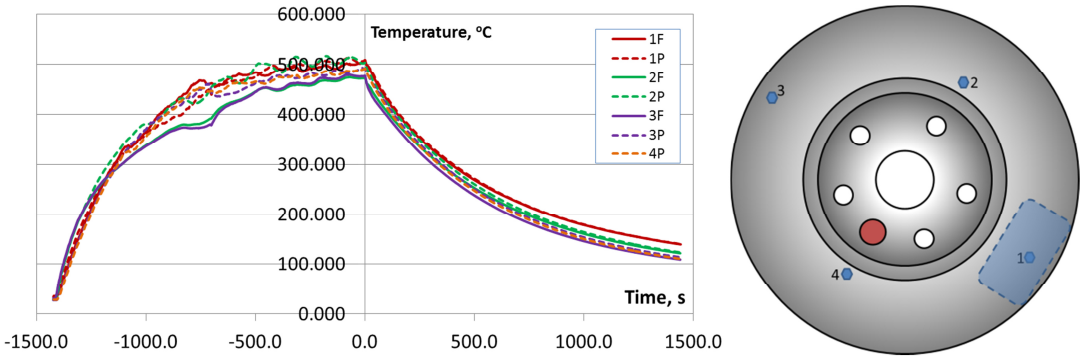

Figure 43. Brake disk temperature measurement points and the temperatures measured

The temperatures of some of the parts, that were not equipped with thermocouples but were still interesting for the investigation, were measured by infrared thermometer and by thermal camera, see Figure 44 for an example of thermal camera image obtained. Using these methods it was found that at the end of heat-up phase tyres have a temperature gradient from 40^0C to 60^0C, and rim surface temperature varies between 90^0C and 130^0C depending on distance from the wheel centre.

Figure 44. An example of thermal image from the experiment

3.3.2 Numerical simulation

The numerical simulation of the brake system performance conducted was just a first step in the process development project that is to be continued and developed. Current model has a large number of limitations and challenges that need to be overcome before a validation of the model can become possible, some of these limitations are summarized below:

- *Model and mesh:* current mesh is simplified with a focus on low cell count, a more detailed model should be used when investigating the effects of the engine bay flows or adding the heat-up phase to the simulation.

- *Initial temperature distribution:* the simulation is currently initialized with the temperature values measured in the wind tunnel, but for simplicity reasons each part is initialised with one homogeneous temperature. This issue will be resolved as soon as the heating-up phase is implemented in the simulation.

- *Material properties:* The simulation model requires a lot of material properties to be defined for all parts and fluids included in the calculations. Such properties as the thermal conductivity and the specific heat need to be defined, preferably with temperature dependant curves. It is especially important for the brake disk and brake pads.

- *Convection modelling:* Fully-transient simulations combining aerodynamics and thermal management are challenging due to significantly different time-steps that should be used. This issue can be solved by freezing the aerodynamic solution and running just thermal simulation for a certain period of time, when significant changes in the airflow are not expected. It should work for the heat-up phase, but in the cool-down phase the flow is driven by the natural convection, and therefore,

the air velocity field is directly affected by the temperatures of different parts. This means that for the soaking phase the airflow needs to be re-computed several times during the simulation. The number of times it should be done for achieving sufficient accuracy needs to be investigated.

- *Radiation modelling:* Radiation model used in the simulation requires emissivity coefficients assigned for every important surface. Defining these coefficients for every surface is extremely challenging task, especially for the brake disk, which is the main participant in radiation heat transfer due to its high temperature. Experimental investigations have shown that the emissivity coefficient for the brake disk surface can be as low as 0.15 or as high as 0.9 depending on the current state of the disk, moreover it may require corrections based on the test case and current temperature [49, 72, 73].

- *Conduction modelling:* Heat transfer from one body to another one is always affected by thermal contact resistance between these bodies. The exact value for this resistance depends on the materials, surface conditions and the contact pressure [74]. It is known that the introduction of thermal contact resistance allows getting better correlation between the experiment and the simulation [75]. Current state of the simulation model does not take this resistance into account, so it requires further investigation.

In its current stage the model allows to do sensitivity studies to identify critical parameters, for example emissivity of the brake disk, see Figure 45, or to do some rough estimations of how different mechanisms of heat transfer are affecting the cool-down of the brakes, see Figure 46.

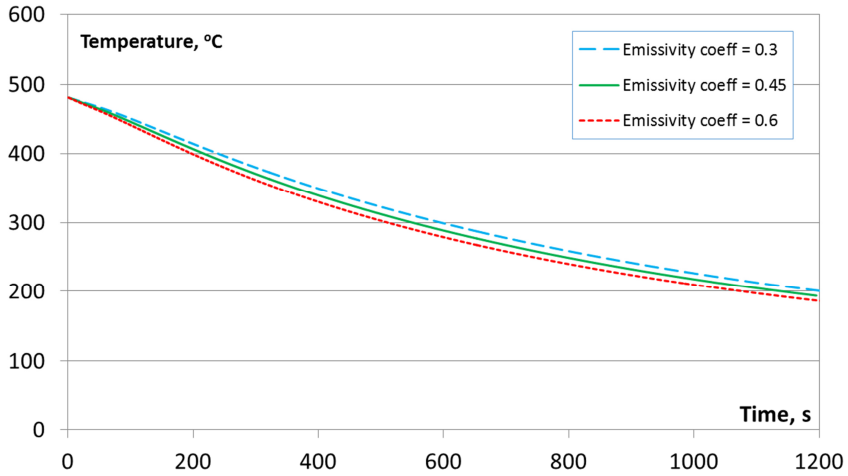

Figure 45. Brake disk (point 3F) temperature estimation depending on emissivity of the disk surface

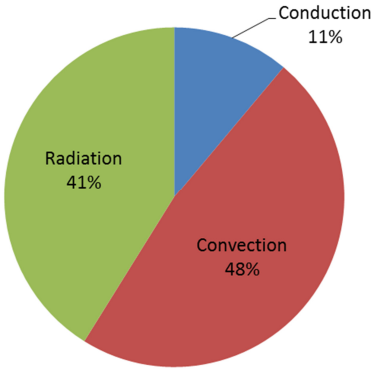

Figure 46. Heat transfer mechanisms for the brake disk cool-down

More details about the experimental and numerical studies within the brake cooling project can be found in Paper IV.

4. Concluding remarks

With the development of computers and increased general engineering knowledge vehicle manufacturers push for more and more advanced methods used in development of their products. This involves not only better experimental equipment and facilities, but also better numerical simulation software and models. Aerodynamics engineers can benefit from it to a large extent since they generally use both experimental and numerical methods. Some of the effects and processes that used to be unaccounted for or were considered of low priority are now being tested and experimented upon.

For example, traditional assumption usually suggests full-size vehicle to be more or less Reynolds-independent in the standard velocity range, but it does not consider changes happening to the vehicle geometry with increasing speed. Moreover, the testing of a full-size passenger vehicle in the wind tunnel usually involves using rigid fastening struts to connect it to the balance. This type of strut allows fixing the vehicle in desired position, but at the same time prevents it from moving in vertical direction. In reality such movement will occur due to aerodynamic lift forces acting on the vehicle body and also due to the wheel centre movement because of inertial expansion of the tyres. It has been shown that having a less fixed option of floating strut, one can achieve a more realistic vehicle body position change due to the velocity. The investigations confirmed that this influences all aerodynamic characteristics of the vehicle including the aerodynamic drag force and hence the aerodynamic drag coefficient.

Another topic that got a lot of attention in recent years is the aerodynamic resistance moment of the wheels, also known as ventilation resistance moment. It has been shown that this moment can be measured experimentally and calculated numerically, and later be included in the driving resistance equation in the form of equivalent ventilation drag force. The investigations indicated that the wheel aerodynamic resistance moment changes significantly with the rim design similarly to the aerodynamic drag force of the vehicle. Both of these parameters need to be taken into account when designing a wheel for a specific vehicle. In this case the total aerodynamic resistance coefficient, that is basically a sum of aerodynamic drag and ventilation resistance coefficients, should be used.

Experimental measurements of the ventilation resistance moment can be done in several different ways; however all of them require large modifications to the vehicle being tested. To measure the wheel aerodynamic resistance moment all other resistances have to be either estimated or eliminated. One of the possible wind tunnel procedures for such measurement was presented in this thesis.

Another possible option to obtain the ventilation resistance values is to use the numerical simulations. It has been shown that different rim designs can be compared against each other in CFD and the experimental trends can be captured. It was also found that the tyre pattern presence and the way the wheel rotation is modelled have a large influence on the ventilation resistance moment calculated. A significant difference was observed when comparing the results obtained using the sliding mesh and different steady-state approaches. The reason behind this difference requires further investigations.

One of the possible ways the engineering research will go in the future is becoming more multidisciplinary and even interdisciplinary. As an example, it can be done by combing aerodynamics and thermal management. In case of the passenger vehicles these two disciplines are interfering in multiple areas and will be merging even more in coming years. This thesis has covered one of such areas, which is brake cooling performance. The investigation conducted included the replication of the Alpine descent brake system test in the Volvo wind tunnel that provided a lot of valuable data for numerical model development and future model verification. First steps in simulation of the same test using CFD software were presented. The investigation showed a large potential, but it still requires a lot of work to be done in order to obtain good correlation between experiment and simulation.

The continuous development of experimental and numerical methods will allow solving tasks with much greater complexity, compared to what was possible several years ago. It will increase the understanding of different processes and allow predicting their results with significantly higher level of accuracy.

5. Summary of papers

This chapter presents a brief summary of the papers appended to the thesis. A quick description is given together with the objective of the investigation and some key results.

***

Paper I
Vdovin, A., Bonitz, S., Landström, C. and Löfdahl, L., "Investigation of Wheel Ventilation-Drag using a Modular Wheel Design Concept," SAE Int. J. Passeng. Cars - Mech. Syst. 6(1):2013, doi:10.4271/2013-01-0953.

This paper describes the methodology used at Volvo Car Corporation aerodynamic wind tunnel to measure the aerodynamic resistance moments (ventilation resistance) of the wheels. The measurement was possible due to a custom–built suspension with a tractive force measurement system installed in the Wheel Drive Units (WDUs). The method described is used to test a number of 17 inch rims and compare them against each other. The study aims at identifying wheel design factors that have significant effect on the ventilation resistance for the investigated wheel size.

The resistance moment is replaced by the equivalent force and the ventilation resistance coefficient is defined. This allowed comparison of total aerodynamic resistance for different rim designs and different velocities. The magnitude of the measured ventilation resistance moment confirms that this effect should be taken into account when designing a wheel. It was found that some of the rim design factors have greater influence on the ventilation resistance than others.

***

Paper II
Vdovin, A., Löfdahl, L., and Sebben, S., "Investigation of Wheel Aerodynamic Resistance of Passenger Cars," SAE Int. J. Passeng. Cars - Mech. Syst. 7(2):2014, doi:10.4271/2014-01-0606.

The paper summarises results of a numerical study of the wheel aerodynamic resistance moment and how it is affected by changing a rim design. This moment is translated into equivalent force and then into equivalent drag coefficient. The changes in this coefficient are compared with the changes happening to aerodynamic drag coefficient. A detailed look is taken at pressure and shear forces acting on the tyre, the rim and the brake disk and how those forces are changing with increased velocity.

The results show the tyres to be the main contributor to the generation of ventilation resistance moment. The rim contribution is found to be largely decreased when the wheel covers are introduced. The rear wheels show a larger potential for improvement both in terms of aerodynamic drag and wheel resistance moment.

***

Paper III
A. Vdovin, L. Löfdahl, S. Sebben and T. Walker, "Investigation of vehicle ride height and wheel position influence on the aerodynamic forces of ground vehicles," in International Vehicle Aerodynamics Conference 2014, Loughborough, UK, 2014.

This paper describes the wind tunnel investigation where the effects of using different types of the vehicle fixation to a force balance are examined. Standard fixed struts are compared to the floating struts that allow vertical displacement of the vehicle body. The visual differences observed include the different shape of the wheel, mainly due to the higher wheel centre, vehicle body lift and pitch angle change. All of these differences are measured by laser displacement transducers and the effects on the drag and lift of the vehicle are investigated both experimentally and numerically.

The results show that the usage of floating struts leads to significant vehicle body position change which in its turn affect all aerodynamic coefficients measured.

***

Paper IV
A. Vdovin, L. Löfdahl and S. Sebben, "Numerical and Experimental Investigations of Brake Cooling for Passenger Cars," in European Conference - Thermal Systems and Aerodynamic Solutions for Ground Vehicles, Torino, Italy, 2015.

This paper summarises some of the findings obtained in a first stage of a large project aimed at reproducing the Alpine descent brake system test procedure using numerical simulations. Firstly, the vehicle is tested in the wind tunnel using the method described in the paper. 140 thermocouples are used to monitor and record temperature history of different parts of the brake system and some parts around it. Both the heat-up and the cool-down phases were conducted in the experimental test. Secondly, this data is used for initialisation of the numerical simulation of the cool-down phase. The procedure used for this simulation is discussed together with a number of challenges and limitations that one needs to face in order to obtain satisfactory correlation of numerical and experimental results.

The cases investigated included control of the under hood cooling fans speeds. It was found that even though these fans are driving the hot air from the engine bay, the introduction of the forced flow during the cool-down phase decreases the cool-down time of brake system parts. The experimental results for the brake fluid, the brake disk and some of other related parts are presented and discussed.

Some of the results of the numerical simulations are presented briefly, including convective airflow calculations and sensitivity study for the brake disk surfaces emissivity coefficient. Numerical simulations are shown to have large potential for improving the knowledge about different processes that cannot be studied experimentally, for example they allow separating the effects of conduction, convection and radiation, and monitoring how their heat transfer rates change with time.

***

Paper V

A. Vdovin, T. Hobeika, L. Löfdahl and S. Sebben, "Numerical Investigations of Aerodynamic Resistance Moments of Rotating Wheels on Passenger Cars," submitted to SAE Int. J. Passeng. Cars - Mech. Syst., 2015.

It was found in paper II and also confirmed by the research of other authors that the tyres are playing an important role in simulation of aerodynamic resistance moment and aerodynamic drag force of the vehicle. This paper investigates the effects of having tyres with tread pattern in the simulation compared to using the slick tyres. Additionally 4 different methods for modelling of the tyre rotation are investigated. Standard rotating wall boundary condition is compared to MRF method used in the first cell around the tyre geometry. The third method involves using MRF approach only inside the groves where the rotating wall boundary condition is unable to provide the correct surface velocities. Finally, the sliding mesh approach is tested and all of the results are compared.

It is shown that for the slick tyres the sliding mesh approach results are very close to the 3 steady-state methods tested; however, this is not the case for the tyres with pattern. The effects of adding the pattern to the tyre are different for different rotation simulation methods used. For all steady-state methods a decrease in ventilation resistance moment is observed for tyres with pattern compared to tyres without it. In contrast, the sliding mesh approach results show an increase in ventilation resistance moment, in some cases reaching values three times higher than the ones obtained using steady-state methods. The reason behind it requires further investigations.

6. References

[1] S. Bonitz, "An investigation into the aerodynamic ventilation drag incurred by wheel rotation on a passenger car, and its influence on the total road load of the car," Master Thesis, TU Berlin, Berlin, Germany, 2012.

[2] "Production statistics," OICA, The International Organization of Motor Vehicle Manufacturers, [Online]. Available: http://oica.net/category/production-statistics/. [Accessed 01 06 2015].

[3] "Climate change and CO2," OICA, International Organization of Motor Vehicle Manufacturers, [Online]. Available: www.oica.net/category/climate-change-and-co2/. [Accessed 02 06 2015].

[4] "Reducing CO2 emissions from passenger cars," European Commission, [Online]. Available: http://ec.europa.eu/clima/policies/transport/vehicles/cars/index_en.htm. [Accessed 02 06 2015].

[5] P. Mock, J. German, A. Bandivadekar and I. Riemersma, "Discrepancies between type-approval and “real-world” fuel-consumption and CO2 values," in *The International Counsil on Clean Transportation*, 2012.

[6] "Worldwide harmonized Light vehicles Test Procedure (WLTP) - Transport - Vehicle Regulations - UNECE Wiki," UNECE, [Online]. Available: www2.unece.org/wiki/pages/viewpage.action?pageId=2523179. [Accessed 16 06 2015].

[7] T. Barlow, S. Latham, S. McCrae and P. Boulter, "A reference book of driving cycles for use in the measurement of road vehicle emissions," TRL limited, 2009.

[8] "DHC-12th session - Transport - UNECE," [Online]. Available: http://www.unece.org/trans/main/wp29/wp29wgs/wp29grpe/wltp_dhc12.html. [Accessed 16 06 2015].

[9] R. Barnard, Road Vehicle Aerodynamic Design, Cornwall, Great Britain: Mechaero Publishing, 2001.

[10] Volkswagen Media Services, "Volkswagen to produce XL1 diesel plug-in hybrid at Osnabrück," 2013. [Online]. Available: http://www.greencarcongress.com/2013/02/xl1-20130221.html. [Accessed 29 04 2013].

[11] S. Bickerstaffe, "Mercedes-Benz B-Class," *Automotive Engineer,* vol. October 2011, pp. 12-13.

[12] W. H. Hucho, "Aerodynamics of Road Vehicles," USA, Society of Automotive Engineers, Inc, 1998.

[13] C. Lueginger, "Neuer Verbrauchszyklus WLTP," in *Haus der Technik*, Munich, Germany, 2014.

[14] M. Pfadenhauer, G. Wickern and K. Zwicker, "On the influence of wheels and tyres on the aerodynamic drag of the vehicles," in *MIRA International Conference on Vehicle Aerodynamics*, 1996.

[15] A. Wagner, "Aerodynamics of a new Audi Q5," in *7th MIRA International Vehicle Aerodynamics Conference* , Warwickshire, UK, 2008.

[16] S. Sebben, "Numerical Simulations of a Car Underbody: Effect of Front-Wheel

Deflectors," in *SAE Technical Paper 2004-01-1307*, 2004.

[17] G. Wickern, K. Zwicker and M. Pfadenhauer, "Rotating Wheels - Their Impact on Wind Tunnel Test Techniques and on Vehicle Drag Results.," in *SAE International (Paper No: 970133)*, Warrendale, PA, 1997 .

[18] A. Wäschle, "The Influence of Rotating Wheels on Vehicle Aerodynamics - Numerical and Experimental Investigations," in *SAE Technical Paper 2007-01-0107*, Detroit, USA, 2007.

[19] P. Elofsson and M. Bannister, "Drag Reduction Mechanisms Due to Moving Ground and Wheel Rotation in Passenger Cars," in *SAE Paper No. 2002-01-0531*, SAE World Congress, 2002.

[20] E. Mercker, N. Breuer, H. Berneburg and H. J. Emmelmann, "On the Aerodynamic Influence Due to Rotating Wheels of Passenger Cars," in *SAE paper No.910311*, 1991.

[21] J. Wiedermann, "The Influence of Ground Simulation and Wheel Rotation on Aerodynamic Drag Optimization - Potential for Reducing Fuel Consumption," in *SAE paper No.960672*, 1996.

[22] G. Wickern and N. Lindener, "The Audi Aeroacoustic Wind Tunnel: Final Design and First Operational Experience," in *SAE Technical Paper 2000-01-0868*, 2000.

[23] J. Sternéus, T. Walker and T. Bender, "Upgrade of the Volvo Cars Aerodynamic Wind Tunnel," in *SAE Technical Paper 2007-01-1043*, 2007.

[24] K. Koremoto, N. Kawamura, N. Kuratani, S. Nakamura, T. Arai, F. Galanga, B. Martindale, E. Duell and S. Muller, "The The Characteristics of the Honda Full Scale Aero-acoustic Wind Tunnel Equipped with a Rolling Road System," in *8th MIRA International Vehicle Aerodynamics Conference 2010 - Low Carbon Vehicles*, Grove, UK, 2010.

[25] K. Tadakuma, T. Sugiyama, K. Maeda and M. Iyota, "Development of Full-Scale Wind Tunnel for Enhancement of Vehicle Aerodynamic and Aero-Acoustic Performance," *SAE Int. J. Passeng. Cars - Mech. Syst.,* vol. 7, no. 2, pp. 603-616, 2014.

[26] A. Cogotti, "The New Moving Ground System of Pininfarina Wind Tunnel," in *SAE Paper No. 2007-01-1044*, 2007.

[27] E. Duell, A. Kharazi, S. Muller, W. Ebeling and E. Mercker, "The BMW AVZ Wind Tunnel Center," in *SAE International conference, Paper No. 2010-01-0118*, 2010.

[28] A. Klemin, "A Belt Method of Representing the Ground," *Journal of Aeronautical Science,* vol. 1, pp. 198-199, 1934.

[29] B. Hetherington and D. Sims-Williams, "Support Strut Interference Effects on Passenger and Racing Car Wind Tunnel Models," in *SAE Technical Paper 2006-01-0565*, 2006.

[30] B. Hetherington and D. Sims-Williams, "Wind Tunnel Model Support Strut Interference," in *SAE Technical Paper 2004-01-0806*, 2004.

[31] C. Landström, L. Löfdahl and T. Walker, "Detailed Flow Studies in Close Proximity of Rotating Wheels on a Passenger Car," *SAE Int. J. Passeng. Cars – Mech. Syst.,* vol. 2, no. 1, pp. 861-874, 2009.

[32] T. Kuthada and J. Wiedemann, "Investigations in a Cooling Air Flow System under the Influence of Road Simulation," in *SAE Technical Paper 2008-01-0796*, Detroit, USA, 2008.

[33] C. Landström, T. Walker, L. Christoffersen and L. Löfdahl, "Influences of Different Front and Rear Wheel Designs on Aerodynamic Drag of a Sedan Type Passenger Car," in *SAE International paper 2011-01-0165*, Warrendale, PA, 2011.

[34] C. Landström, L. Josefsson, T. Walker and L. Löfdahl, "An experimental investigation of wheel design parameters with respect to aerodynamic drag," in *FKFS Conference*, Stuttgart, Germany, 2011.

[35] C. Landstrom, L. Josefsson, T. Walker and L. Lofdahl, "Aerodynamic Effects of Different Tire Models on a Sedan Type Passenger Car," *SAE Int. J. Passeng. Cars - Mech. Syst.,* vol. 5, no. 1, pp. 136-151, 2012.

[36] P. Mlinaric and S. Sebben, "Investigation of the Influence of Tyre Deflection and Tyre Contact Patch on CFD Predictions of Aerodynamic Forces on a Passenger Car," in *MIRA International Conference on Vehicle Aerodynamics*, Coventry, England, 2008.

[37] T. Hobeika, S. Sebben and C. Landstrom, "Investigation of the Influence of Tyre Geometry on the Aerodynamics of Passenger Cars," *SAE Int. J. Passeng. Cars - Mech. Syst.,* vol. 6(1), no. doi:10.4271/2013-01-0955., pp. 316-325, 2013.

[38] T. Hobeika, L. Lofdahl and S. Sebben, "Study of different tyre simulation methods and effects on passenger car aerodynamics," in *International Vehicle Aerodyanmics Conference*, Loughborough, UK, 2014.

[39] W. Mayer and J. Wiedemann, "The Influence of Rotating Wheels on Total Road Load," in *SAE Paper No. 2007-01-1047*, SAE World Congress, 2007.

[40] F. Modlinger, R. Demuth and N. Adams, "New Directions in the Optimization of the Flow around Wheels and Wheel Arches," in *MIRA International Conference on Vehicle Aerodynamics*, Coventry, England, 2008.

[41] C. Landström, S. Sebben and L. Löfdahl, "Effects of wheel orientation on predicted flow field and forces when modelling rotating wheels using CFD," in *8th MIRA International Vehicle Aerodynamics Conference*, 2010.

[42] A. Vdovin, S. Bonitz, C. Landstrom and L. Lofdahl, "Investigation of Wheel Ventilation-Drag using a Modular Wheel Design Concept," *SAE Int. J. Passeng. Cars - Mech. Syst.,* vol. 6, no. 1, 2013.

[43] M. Stellato, "FCA Full Scale Wind Tunnel upgrade: “5-belts” rolling Road Simulation System and first Results," in *Thermal Systems and Aerodynamic Solutions for Ground Vehicles*, Torino, Italy, 2015.

[44] E. Palmer, R. Mishra, J. Fieldhouse and J. Layfield, "Analysis of Air Flow and Heat Dissipation from a High Performance GT Car Front Brake," in *SAE Technical Paper 2008-01-0820*, 2008.

[45] G. Barigozzi, A. Perdichizzi and M. Donati, "Combined Experimental and CFD Investigation of Brake Discs Aero-thermal Performances," *SAE Int. J. Passeng. Cars - Mech. Syst.,* vol. 1, pp. 1194-1201, 2009.

[46] S. Reddy, J. Mallikarjuna and V. Ganesan, "Flow and Heat Transfer Analysis of a Ventilated Disc Brake Rotor Using CFD," in *SAE Technical Paper 2008-01-0822*, 2008.

[47] S. Yigit, P. Penther, J. Wuchatsch and F. Werner, "A Monolithic Approach to Simulate the Cooling Behavior of Disk Brakes," *SAE Int. J. Passeng. Cars - Mech. Syst.,* vol. 6(3), pp. 1430-1437, 2013.

[48] B. Choi, J. Park and M. Kim, "Development of the Virtual Test Technology for Evaluating Thermal Performance of Disc Brake," in *SAE Technical Paper 2009-01-*

0857, 2009.

[49] G. Voller, M. Tirovic, R. Morris and P. Gibbens, "Analysis of automotive disc brake cooling characteristics," *Proceedings of the Institution of Mechanical Engineers, Part D: Journal of Automobile Engineering,* vol. 217, pp. 657-666, 2003.

[50] H. Sun, "Sensitivity Study on Brake Cooling Performance," in *SAE Technical Paper 2006-01-0694*, 2006.

[51] T. Schuetz, "Cooling Analysis of a Passenger Car Disk Brake," in *SAE Technical Paper 2009-01-3049*, 2009.

[52] A. Stephens, S. Watkins and C. Dixon, "Aerodynamic Testing of a Vented Disc Brake," in *SAE Technical Paper 2003-01-0932*, 2003.

[53] D. Mukutmoni, S. Jelic, J. Han and M. Haffey, "Role of Accurate Numerical Simulation of Brake Cooldown in Brake Design Process," *SAE Int. J. Passeng. Cars - Mech. Syst.,* vol. 5(4), pp. 1199-1210, 2012.

[54] Z. Qiu, C. Landström, L. Löfdahl and L. Josefsson, "Wheel Aerodynamic Developments on Passenger Cars by Module-based Prototype Rims and Stationary Rim Shields," in *FISITA World Automotive Congress*, Budapest, Hungary, 2010.

[55] B. Schnepf, G. Tesch and T. Indinger, "On the Influence of Ride Height Changes on the Aerodynamic Performance of Wheel Designs," in *JSAE Annual Congress*, 2014.

[56] "ANSA pre-processor," BETA CAE Systems S.A., [Online]. Available: http://www.beta-cae.com/ansa.htm. [Accessed 01 06 2015].

[57] "STAR-CCM+® | CFD Simulation Software," CD-adapco, [Online]. Available: http://www.cd-adapco.com/products/star-ccm%C2%AE. [Accessed 01 06 2015].

[58] ANSYS, "Fluent Productivity Tools for CHT Simulations," 2015.

[59] "ANSYS Fluent," ANSYS, [Online]. Available: http://www.ansys.com/Products/Simulation+Technology/Fluid+Dynamics/Fluid+Dynamics+Products/ANSYS+Fluent. [Accessed 01 06 2015].

[60] "Harpoon extreme mesher," Sharc Ltd, [Online]. Available: http://www.sharc.co.uk/. [Accessed 01 06 2015].

[61] "EnSight," Computational Engineering International, Inc. (CEI Inc.), [Online]. Available: https://www.ceisoftware.com/. [Accessed 01 06 2015].

[62] Z. Chroneer, "The CFD Process for Aerodynamics at Volvo Cars using Harpoon-Fluent," in *3rd European Automotive CFD Conference*, 2007.

[63] ANSYS Inc, "ANSYS Fluent User's Guide," Canonsburg, PA, 2013.

[64] CD-adapco, "Star-CCM+ User Guide," 2014.

[65] F. Makowski and S. Kim, "Advances in External-Aero Simulation of Ground Vehicles Using the Steady RANS Equations," in *SAE Technical Paper 2000-01-0484*, 2000.

[66] T. Shih, W. Liou, A. Shabbir, Z. Yang and J. Zhu, "A New k-e Eddy-Viscosity Model for High Reynolds Number Turbulence Flows - Model Development and Validation," *Computers & Fluids,* vol. 24, no. 3, pp. 227-238, 1995.

[67] A. Cogotti, "Aerodynamic characteristics of car wheels," *International Journal of Vehicle Design, Special Publications SP3,* pp. 173-196, 1983.

[68] J. Fabijanic, "An experimental Investigation of Wheel-Well Flows," in *SAE Paper 960901*, 1996.

[69] C. Landström, T. Walker, L. Christoffersen and L. Löfdahl, "Influences of Different

Front and Rear Wheel Designs on Aerodynamic Drag of a Sedan Type Passenger Car," in *SAE International*, Warrendale, PA, 2011.

[70] O. Danielsson, J. Gillberg, K. Narendra, R. Ryrholm and H. Zein, "Report: Brake Cooling - Automotive Engineering Project," Chalmers University, 2015.

[71] G. Gigan, T. Vernersson, R. Lundén and P. Skoglund, "Disc brakes for heavy vehicles: an experimental study of temperatures and cracks," *Journal of Automobile Engineering,* vol. 229, no. 6, pp. 684-707, 2015.

[72] R. Eisengräber, J. Grochowicz, M. Schuster and K. Augsburg, "Comparison of Different Methods for the Determination of the Friction Temperature of Disc Brakes," in *SAE Technical Paper 1999-01-0138*, 1999.

[73] G. Dragomir, R. Pancu, C. Bungau, H. Beles and L. Georgescu, "Studies About Emissivity Variation Depending On The Temperature For Car Brake Disc," *Annals Of The Oradea University: Fascicle Of Management And Technological Engineering,* no. 1, pp. 253-256, 2014.

[74] M. Yovanovich, "Four Decades of Research on Thermal Contact, Gap, and Joint Resistance in Microelectronics," *Ieee Transactions On Components And Packaging Technologies,* vol. 28, no. 2, pp. 182-206, 2005.

[75] K. Narendra Babu, "Thermal Contact Resistance: Experiments and Simulation," Master’s thesis in Automotive Engineering, Chalmers, 2015.

Part II
Appended Papers